TI Designs

1-g Resolution Over 15-kg Range Sub-100-nV$_{PP}$ Noise Front-End Reference Design for Weight and Vibration Measurement

TEXAS INSTRUMENTS

TI Designs

The TIDA-00765 is a less than 100-nV$_{PP}$ noise analog front-end that reads out resistive load cells for weight and vibration measurement. It is ideally suited for appliances that require high resolution due to a large dynamic range or considerable weight offset.

As an example, this design is integrated into an advanced food processor to showcase its capability to resolve 1 g for a 15-kg food processor during significant levels of switching supply noise and rapid temperature changes. Drift and interference are common issues in this harsh environment. In this design, these are suppressed by significant filtering and AC bridge excitation to consistently achieve high performance. This design is based on the high-resolution ADS1220 delta-sigma ADC.

This robust circuit reference design includes theory, component selection, PCB design, example code, and measured performance data.

Design Resources

TIDA-00765	Design Folder
ADS1220	Product Folder
LP5907	Product Folder
MSP430G2553	Product Folder
TS5A21366	Product Folder
TPD4E1U06	Product Folder
CSD23381F4	Product Folder
CSD13381F4	Product Folder
LMT01	Product Folder

ASK Our E2E Experts

Design Features

- Provides Bridge Excitation and Reads Multiple and Individual Wheatstone Bridges or Strains Gauge-Based Load Cells
- Performance in Weighing Mode
  - <100-nV$_{PP}$ Noise With Sliding Average for 50-mV Input Range ↔ Down to 5-ppm Resolution
  - Settling Time of 1 Second
  - Response Time of 125 ms
  - >15,000 Noise-Free Count Weigh-Scale Solution for 1-mV/V Gauges
  - <5-µV Total Error From 0°C to 85°C
  - AC Excitation Cancels Temperature Drift of Parasitic Thermocouples and Other Offsets
- Captures Vibrations up to 500 Hz
- Robust Low-Noise Performance in Face of 500-mV$_{PP}$, 100-kHz Switching Supply Noise
- Firmware Provides ADS1220 Example Code

Featured Applications

- Weight and Vibration Measurement for Appliances Such as
  - Food Processors, Mixers, and Blenders
  - Microwaves and Ovens
  - Cooking Ranges
- Weight Measurement for Equipment With High-Resolution Requirements Due to Dynamic Range or Considerable Weight Offset
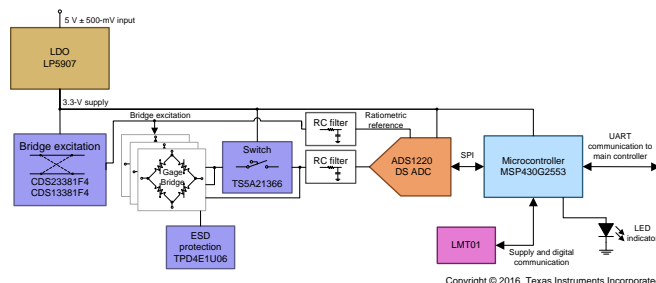
All trademarks are the property of their respective owners.

1-g Resolution Over 15-kg Range Sub-100-nV$_{PP}$ Noise Front-End Reference Design for Weight and Vibration Measurement

Copyright © 2016, Texas Instruments Incorporated

An IMPORTANT NOTICE at the end of this TI reference design addresses authorized use, intellectual property matters and other important disclaimers and information.

1 System Description

This design demonstrates the ease and advantages of designing a cost effective and 100-nV$_{PP}$ high-resolution analog front-end (AFE) to integrate high-resolution, 5-ppm weighing and vibration detection capabilities into smart household appliances.

Appliances have eased household work and freed up time for more important activities. Recently, new features and functionality are emerging that make smart appliances more helpful and autonomous. This trend reaches small household appliances like food processors, mixers, and blenders. Among the new features is the integration of weighing capabilities into mixers, cook fields, cookers, microwaves, and other appliances.

Figure 1 shows an example of an advanced food processor. This food processor consists of a main body and interchangeable electric motor-driven attachments and bowls. Integrated heating elements generate heat to facilitate cooking. A central MCU controls the motor and heater for guided cooking programs. For such guided programs, smarter food processors can relieve their users from repetitive and boring control tasks and operate autonomously.
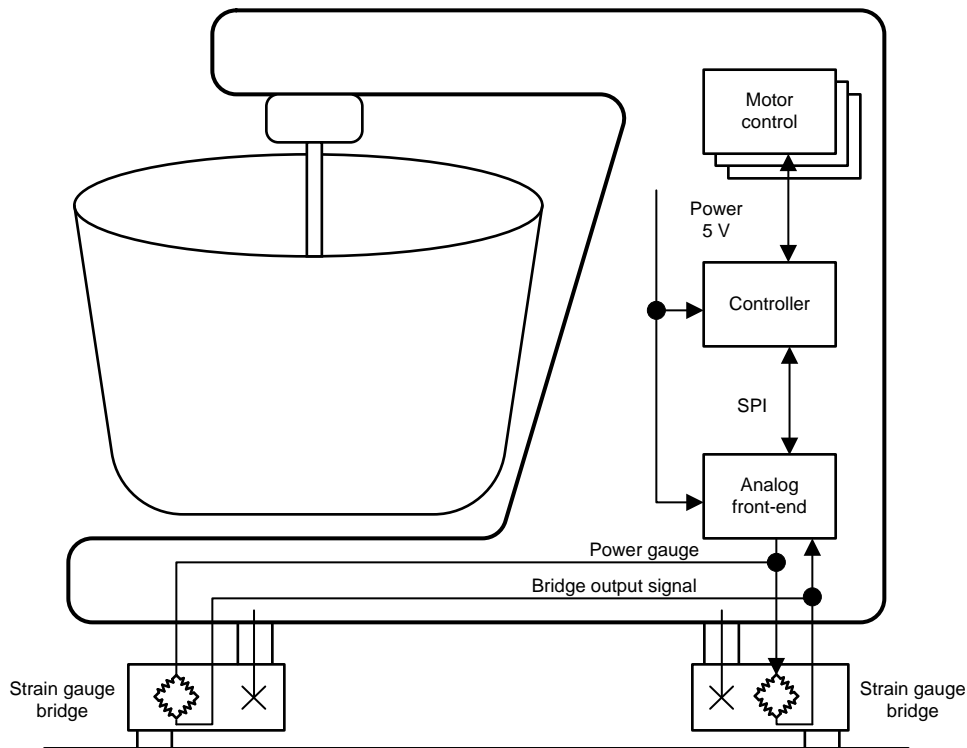
Copyright © 2016, Texas Instruments Incorporated

Figure 1. Food Processor Including Supply, Controllers, Weight Cells, and AFE

If the functionality of the kitchen scale is integrated into the mixer, this significantly eases the dosage of ingredients or enables control, for example thickening sauces. If the detection of mixers vibrations is integrated, it enables the mixer to become smarter and to regulate the operation speed to:

- Keep vibrations within limits in case of unbalances to ensure safe yet effective operation
- Keep the level of audible noise reasonably
- Detect and react to the progress of food processing

To measure weight and vibrations, a load cell and strain gauge bridges are integrated into each foot of the mixer. The total weight is the sum of the weight of the mixer, attachments, and food. This weight bends the load cells, expands or compresses the strain gauges, and decreases or increases their resistance. The resistive strain gauges are configured in a bridge configuration and produce a DC voltage proportional to the momentary weight across their outputs when supplied with a DC voltage. The AFE reads the weight output sensor bridge accurately with the ADS1220, a high-resolution, inherently highly-linear delta-sigma ADC. The high level of the converters' integration guarantees the specified high accuracy of the conversion results. The ultra-low-power MSP430G2553 mixed-signal microcontroller controls the operation of the AFE and ADS1220 either in weighing or vibration detection mode.

In weighing mode, high resolution is a must as the weight of recipe ingredients needs to be measured with < 1g accurately against the huge systematic offset of the total weight of the mixer of up to 20 kg. To minimize the drift of the strain gauges in weight measurement mode, the MSP430G2553 microcontroller periodically changes the polarity of the excitation voltage of the strain gauge bridge between measurements. This periodical polarity reversal chops the bridge and consequently removes offsets and, more importantly, the offset drifts from the conversion result [1]. The AFE filters and suppresses the electromagnetic interferences picked up in the harsh environment. The MSP430G2553 microcontroller computes the actual weight reading from the raw data of the ADS1220 and can compensate for non-idealities like nonlinearity and temperature drift of cost-effective strain sensor cells. The reading is transmitted by the MSP430G2553 microcontroller from the AFE to the main processor through UART.

In vibration detection mode, high sample rates are required while the resolution requirements are relaxed. Therefore, the MSP430G2553 microcontroller maintains the polarity of the bridge excitation, saves associated settling times, and runs the ADS1220 at its highest sampling rate to quantify the transient movements of the mixer to the Nyquist frequency of the motor's rotation. To maximize the sensitivity towards careening movements, only a single load cell is read out in this mode by the ADS1220. In this case, this avoids the unwanted averaging effects over the mixer feet.

Due to the harsh environment of switching regulators and motors, the supply of the AFE supply is extremely noisy. To combat significantly large signal disturbances, the low-dropout (LDO) regulator LP5907 creates in face of significantly large signal disturbances a clean supply voltage with 6.5 μV_{RMS}. This supply voltage is due to its excellent power supply rejection of > 60 dB to high frequencies above 100 kHz in the face of driving the low ohmic strain gauge bridge sensors with load currents of 40 mA.

2 Key System Specifications

The AFE requirements are derived from the system requirements of a weight scale of an advanced food processor. First, consider the system operation conditions and system requirements and then consider the AFE requirements. Moreover, as the requirements of the weight and vibration measurement modes are fundamentally different, the requirements for these modes are treated separately.

First, the conditions of the weight scale operation and general system requirements are defined in Table 1. The weight scale needs to operate indoors over a temperature range from 0°C to 85°C. It is supplied from a noisy 100-kHz switching supply with 5 V with perturbations of up to ±500 mV$_{PP}$, mainly at the switching and line frequency. The sensitivity of the weight scale strain gauge bridges is assumed to be 5 mV/V over a full scale of 5 kg per foot (typically) and a resistance of 350 Ω. The sensitivity of the weight scale strain gauge bridge configuration is 1 mV/kg, as discussed in Section 4. The total weight to be measured of the food processor, attachments, and food does not exceed 15 kg total.

NOTE: Though a sensitivity of 5 mV/V for individual load cells is assumed, the design supports sensitivities down to 1 mV/V with a reduced margin.

Table 1. Operation Conditions and General System Requirements

PARAMETER	SPECIFICATION
Temperature range	0°C to 85°C
Nominal supply voltage	5 V
Supply voltage ripple	Up to ±500 mV$_{PP}$ at 100 kHz and 50 or 60 Hz
Sensitivity of single gauge bridge	5 mV/V typ ±10% for full scale of 5 kg
Sensitivity of bridge configuration	1 mV/kg
Resistance of bridges	350 W
Total weight range	Up to 20 kg
Operation modes	Weight measurement Vibration measurement

Second, the system requirements in weight measurement mode are enumerated in Table 2. The display resolution is 1 g and this reading is stable. An 8-kg step measurement is reproducible to ±5 g. The drift of the weight reading is less than ±20 g for a temperature change of 10°C. The readings are not affected by the disturbances mentioned in Table 2 at the switching or line frequency with the ±500-mV$_{PP}$ bonds defined in Table 1. To provide a good trade-off between sufficient filtering and user experience, the sample rate is 8 SPS to respond rapidly upon weight changes; the moving average of the reading settles within 1 second.

Table 2. System Requirements in Weight Measurement Mode

PARAMETER	SPECIFICATION
Resolution of reading	Stable 1-g reading
Reproducibility	±10 g for a weight step of 2 kg
Temperature drift	±25 g over DT = 10°C
Robustness to disturbances at 50 or 60-Hz line frequencies	No disturbance of stable reading
Robustness to disturbances at operation frequency f$_{SW}$ of switching supply at 100 kHz	No disturbance of stable reading
Sample rate	8 SPS every 125 ms
Reading settling	Within 1 sec

4 *1-g Resolution Over 15-kg Range Sub-100-nV$_{PP}$ Noise Front-End Reference Design for Weight and Vibration Measurement*

TIDUBL0A–April 2016–Revised June 2016
Submit Documentation Feedback

AFE requirements in weight measurement mode are summarized in Table 3. The maximum weight and sensitivity of the bridge defines the input range of the AFE to be within 22 mV. For a stable reading, the peak-to-peak noise of the reading needs to be below 0.5 µV. The reading noise remains below this limit against supply noises up to ±500-mV$_{PP}$ at the switching frequency of 100 kHz and at the line frequency of 50 or 60 Hz. For reproducibility, a reading must be within an error of ±10 µV after an 8-mV step. The temperature drift of the reading must be below ±10 µV for a temperature change of 10°C. To capture the total weight of the mixer, a weight capture with a single channel is sufficient. The requirements for sampling rate and settling are identical with the system requirements in weight measurement mode, the sample rate is 8 SPS and the reading settles within 1 second. To minimize the drift of the strain gauges, each reading is derived as the average of the capture of the bridge output before and after polarity reversal of the bridge excitation. This excitation reversal facilitates chopping at bridge level and reduces the drift of the resistive strain gauge [1]. Moreover, two LEDs indicate a status as proper AFE operation. To meet the cost and space constraints the printed circuit board (PCB) has no more than two layers and an area below 8 cm^2.

Table 3. AFE Requirements in Weight Measurement Mode

PARAMETER	SPECIFICATION
Maximum input range	< 22 mV
Peak-to-peak noise	<0.5 µV$_{PP}$ within 1 s for sliding average
	For up to ±500-mV$_{PP}$ supply noise at 100 kHz and 50 or 60 Hz
Reproducibility	±10 µV for 8-mV step
Temperature drift	±10 µV over DT= 10°C
Number of channels	Single channel
Sample rate	8 Hz every 125 ms
Reading settling	Within 1 sec (mov avg)
Bridge excitation	AC excitation
Number of LEDs or PWM channels	2 LEDs indicating operation
Cost effective PCB	2-layer PCB < 8 cm^2

Third, the system requirements in vibration measurement mode are specified in Table 4. The resolution of the vibration measurement detects forces below 0.1 N. To sample well above the Nyquist rate of the rotations, which is up to 250 s^{-1} of a typical mixer, the sample rate is 1 kSPS and the bandwidth is greater than 500 Hz.

Table 4. System Requirements in Vibration Measurement Mode

PARAMETER	SPECIFICATION
Resolution of reading	0.1-N horizontal unbalance
Sample rate	1 kSPS
Bandwidth	>500Hz

AFE requirements in vibration measurement mode are listed in Table 5. The maximum input range remains below 22 mV. The peak-to-peak noise is well below 10 μV_{PP}. Due to the careening movement associated with unbalances during the rotation, the capture of the force of a single foot or strain gauge of the mixer is in this case sufficient. The 1-kSPS sample rate and 500-Hz bandwidth requirements are identical with the weight scale system requirements.

Table 5. AFE Requirements in Vibration Measurement Mode

PARAMETER	SPECIFICATION
Maximum input range	< 22 mV
Peak-to-peak noise	<10 μV_{PP}
Number of channels	Single channel
Sample rate	1 kSPS
Bandwidth	> 500 Hz

1-g Resolution Over 15-kg Range Sub-100-nV$_{PP}$ Noise Front-End Reference Design for Weight and Vibration Measurement

3   System Design Theory

3.1   *Resistive Strain Gauge Bridge Weight Measurements*

The most common technique to convert weight into an electrical signal is to use a resistive load cell configured as a Wheatstone bridge. In this configuration, one or more of the resistors change value in proportion to the load (weight) applied. To measure this effect, an excitation voltage V_{EXC} (or current) source is applied across the top and bottom of the bridge and the output signal V_{OUT} is measured as the differential voltage across the middle nodes, as shown in Figure 2 [5].
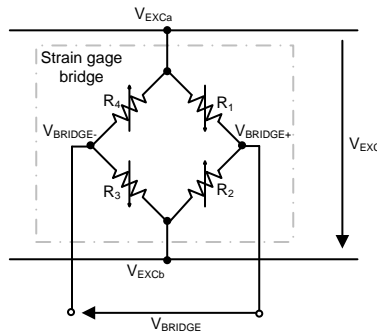
Copyright © 2016, Texas Instruments Incorporated

Figure 2. Wheatstone Bridge

In practice, load cells are specified with a known sensitivity (or rated output) and a rated capacity (maximum load). The sensitivity is specified by the ratio of the output voltage produced per 1-V excitation voltage (given in units of mV/V) with the rated capacity load applied. The full-scale output voltage of the load cell is then calculated by Equation 1:

$$V_{BRIDGE}\left(mV\right) = \text{Sensitivity}_{BRIDGE}\left(\frac{mV}{V}\right) \times V_{EXC}\left(V\right)$$

(1)

For example, a 5-mV/V load cell excited with 3.3 V will have a full-scale output voltage of 16.5 mV. Note that the magnitude of the output signal is directly proportional to the magnitude of the excitation voltage and applied load. In general, the output voltage for any other applied load will scale linearly from no load to the maximum load. (Bridge linearization techniques may be used to increase the bridge linearity, but this topic is outside the scope of this TI Design) [5].

3.2 Ratiometric Bridge Measurement

The voltage-excited bridge is connected to the ADC using a ratiometric connection, as shown in Figure 3.
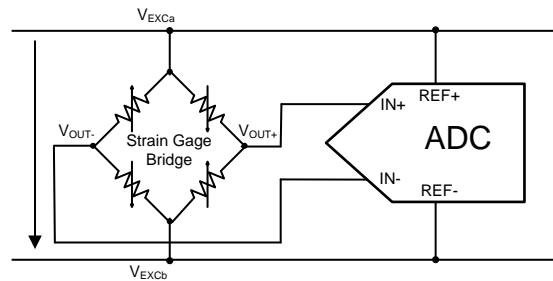
Copyright © 2016, Texas Instruments Incorporated

Figure 3. Ratiometric Bridge Configuration

In this configuration, the bridge excitation voltage is used as the ADC's reference voltage. Any changes in the bridge excitation voltage, due to temperature drift or noise, affect both the input signal and reference proportionately. Therefore, the ADC conversion results (codes) remain unaffected by changes in the excitation or reference voltage, as shown by Equation 2.

$$N_{CONV} \propto \frac{V_{BRIDGE}}{V_{EXC}} = \frac{Load \times Sensitivity \times V_{EXC}}{V_{EXC}} = Load \times Sensitivity$$

(2)

Another benefit of ratiometric bridge measurements is that reference noise is reduced because the reference noise is common to both the ADC and reference inputs. To the degree that the reference noise seen by the ADC input and reference terminals match, reference noise is ratiometrically removed from the ADC conversion results, as Equation 2 shows. Therefore, match input and reference filters to provide the best reference noise rejection (discussed in SBAA201) [5].

3.3 Resistive Bridge Configurations

For mechanical stable stance and upright orientation, the food processor needs to have at least 3 feet, as a plane is well defined by three points. Therefore, the weight of the food processor will be distributed over at least 3 feet. As the different requirements for weight and vibration measurement translate into different configurations, each case is considered separately.

An accurate weight measurement requires measuring the gravitational force in each foot, as the balance point of a food processor varies depending on the attachments and load, so the gravitational force will rarely be equally divided between the feet. Consequently, each foot requires a strain gauge to capture the sum of all gravitational forces. To measure the absolute total weight, average the output signals of these strain gauges.

The most cost effective approach to averaging the output signal of the strain gauges is to short the respective terminals of the different bridges with each other and use the bridges in a parallel configuration as depicted in Figure 4. This solution saves the cost of additional amplifiers or acquisition channels. With a summing amplifier, the sensitivity of the bridge configuration could be increased, but this is not required to achieve the desired resolution.
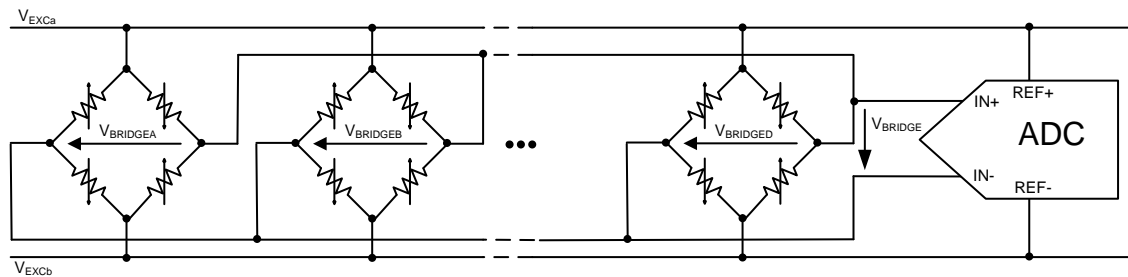
Copyright © 2016, Texas Instruments Incorporated

Figure 4. Parallel Configuration

The sensitivity of this configuration corresponds to the change of the output voltage of the parallel connection (V_{BRIDGE}) divided by the load. The maximum output voltage is the sensitivity of a single gauge times its excitation voltage. The maximum load is the product of the number of the gauges times the maximum rated load of a single gauge. Therefore, expect a sensitivity of the parallel configuration of 1 mV/kg as indicated in Equation 3.

$$\text{Sensitivity}\left(\frac{mV}{kg}\right) = \frac{V_{BRIDGE}(mV)}{\text{Load}(kg)} = \frac{\text{Sensitivity}_{BRIDGE}\left(\frac{mV}{V}\right) \times V_{EXC}(V)}{(\text{Gage count}) \times (\text{Max gage load})} = \frac{4.5\frac{mV}{V} \times 3.3\,V}{3 \times 5\,kg} \approx 1\frac{mV}{kg}$$ (3)

The aim of measuring the vibrations of a food processor is fundamentally different from the weight measurement. In this case, the measurement of the dynamic changes caused by unbalances or impulses from the actual processing is of interest. Due to the rotationally symmetric nature of the careening and reeling movements of the mixer, an average between the feet is counterproductive and undesirable to quantify the vibrations; however, due to the symmetric nature of the movement, it is sufficient to capture the force variations of a single foot.

The capability to measure either weight or vibration requires the user to measure either all feet or an individual foot. It can be introduced with low-ohmic, low-leakage switches as depicted in Figure 5 into the bridge output signal path. In the weight measurement mode, the mode switches are closed, all bridges are shorted, and the ADC captures the average signal of all feet. In vibration measurement mode, the mode switches open and the ADC is connected to a single bridge output.
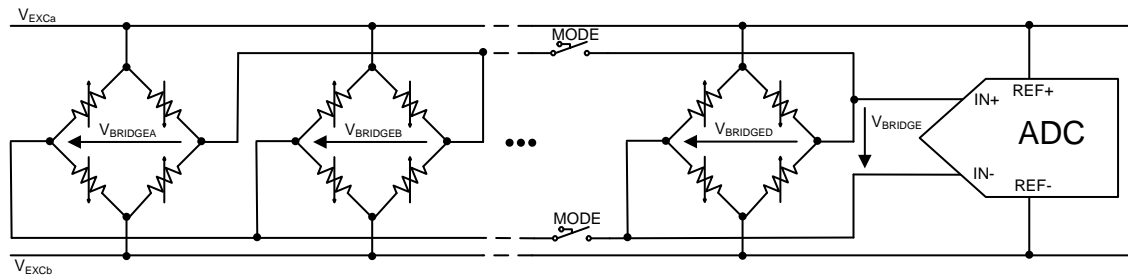
Figure 5. Modified Parallel Configuration

3.4 AC Excitation

Almost every high-resolution design capturing absolute quantities is concerned with temperature drift. In the following section, AC excitation is introduced to reduce such drift and keep it over production tolerances under robust, tight control.

3.4.1 General Principle of Input Chopping

Chopping is a form of averaging that samples a differential input from both directions and averages the conversion results. Figure 6 shows the two phases of an ADC sampling a chopped input with system offset voltages modeled as V_{OS1} and V_{OS2}.
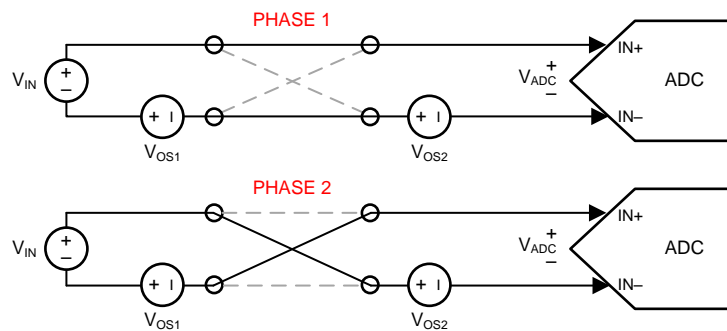
Figure 6. Input Chopping Concept [5]

Many high-resolution ADCs, such as the ADS1262, integrate input chopping into the device to reduce the offset and offset drift of the ADC. By performing the chopping operation, any systematic offsets that occur after the chopping circuitry (primarily the ADC's offset) are removed, as shown by Equation 4.

$$V_{ADC} = \frac{V_{ADC}(PHASE\,1) - V_{ADC}(PHASE\,2)}{2} = \frac{(V_{IN} + V_{OS1} + V_{OS2}) - (-V_{IN} - V_{OS1} + V_{OS2})}{2} = V_{IN} \tag{4}$$

Systematic offsets that occur before the input chopping circuitry (represented by V_{OS1}) are not removed by chopping. These offsets are seen as part of the differential input signal and are only removed by offset calibration. However, slowly changing offsets that occur after the chopping (represented by V_{OS2}) are dynamically removed.

> **NOTE:** This design does not use the ADC's input chopping feature. This discussion is provided only to introduce the input chopping concept and how it works as a prerequisite for understanding AC bridge excitation [5].

3.4.2   AC Bridge Excitation

AC bridge excitation is an extension of input chopping. While input chopping only reduces the offset and offset drift of the ADC, AC bridge excitation reduces the offset and offset drift of the whole measurement system. AC bridge excitation performs the same operation as ADC input chopping, but performs the chopping directly on the bridge sensor. Recalling the observation from Section 3.4.1 that offsets after the chopping stage are removed, it is then most beneficial to place the chopping circuitry as close to the sensor output as possible. By doing so, the measurement system's offset is almost completely removed from the measurement results.

AC bridge excitation does not excite the bridge with an actual AC signal (as the name would seem to imply). AC bridge excitation is performed by applying a DC excitation voltage to the bridge and alternating the polarity of the excitation voltage, as seen in Figure 7.
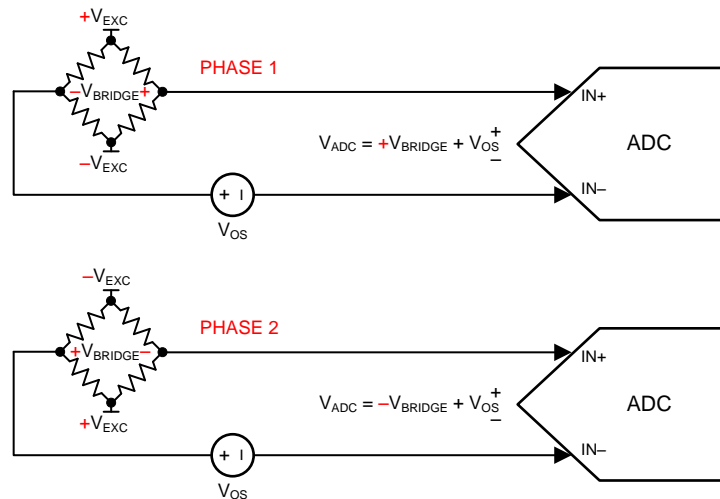
Figure 7. AC Bridge Excitation Concept [5]

Equation 5 shows that AC bridge excitation removes offsets in the same way that input chopping removes offsets. The only difference between these two methods is the location of the chopping and switching.

$$V_{ADC} = \frac{V_{ADC}(PHASE\,1) - V_{ADC}(PHASE\,2)}{2} = \frac{(V_{BRIDGE} + V_{OS}) - (-V_{BRIDGE} + V_{OS})}{2} = V_{BRIDGE}$$

(5)

The offset voltage, V_{OS}, of Figure 7 comprises all offset voltages in the measurement system. These may include the ADC's offset, parasitic thermocouples (to be discussed in Section 3.4.3), or any offsets added by signal conditioning circuitry. Therefore, as long as V_{OS} changes slowly (with respect to the chopping frequency), the system's offset and offset drift are dynamically removed.

The effect of AC bridge excitation is much like continuously measuring and applying a system offset calibration (removing the overall offset of the measurement system, as opposed to input chopping, which only removes the ADC's contribution to the system offset).

Note that applying the AC bridge excitation technique will require the reference connections to be switched to keep the reference voltage (as seen by the ADC) positive.

3.4.3 Overview of Causes of Offset and Offset Drift

Thermocouples are a very useful and common type of temperature sensor. They are formed by junctions of dissimilar metals. When these junctions are exposed to temperature gradients, a thermal electromotive force (EMF), or Seebeck voltage, is produced as a function of the temperature gradient and the metals involved. When thermocouples are used intentionally, they can provide accurate temperature sensing over a wide temperature range and at a low cost. However, unintentional thermocouples are just as common (if not more so) and can greatly reduce the accuracy of precision sensing applications. When used unintentionally, this guide refers to these thermocouples as parasitic thermocouples.

See previous TI Design documents (SLAU509 or TIDU574) for more detailed descriptions and overviews of thermocouple theory.

Parasitic thermocouples exist in many locations within a circuit. Most connections to the PCB will involve multiple dissimilar metals such as copper, tin, lead, nickel, gold, silver, aluminum, and so on. The larger the Seebeck coefficient (or sensitivity, expressed in µV/°C) between these junctions, the larger the offset voltage that can be introduced into the circuit as a temperature gradient is formed. The typical thermocouple sensitivity of most dissimilar metals will have a Seebeck coefficient in the range of a few microvolts per degree Celsius (µV/°C). However, thermocouples with sensitivities >500 µV/°C are possible with copper-copper oxide junctions (caused by oxidation).

Parasitic thermocouples add to the offset and offset drift of the measurement system and may significantly degrade the overall system accuracy.

3.4.3.1 Reducing the Effects of Parasitic Thermocouples

PCB layout can reduce the effects of parasitic thermocouples. Symmetrical PCB layouts and differential measurements may help to match parasitic thermocouples and cancel any common-mode offsets. The use of a large (solid) ground plane can also act as a heat sink to remove thermal gradients. By keeping dissimilar metal junctions at a constant temperature, the parasitic thermocouple will not induce any additional Seebeck (offset) voltage because of the law of intermediate metals.

Calibration may also be performed to correct for these offsets under certain conditions; however, dynamically changing environments may result in dynamic offsets, which are difficult to correct by calibration alone. Even when calibrations are performed at multiple operating temperatures, the effect of parasitic thermocouples may still be observed as an offset drift over temperature.

AC bridge excitation is one of the best methods to remove the effects of parasitic thermocouples. Parasitic thermocouples appear after the chopping stage; therefore, their offset is continuously removed. This is the advantage of AC bridge excitation when compared to offset calibration, which can only remove the initial offset.

3.4.3.2 Other Causes of Offset and Offset Drift

Parasitic thermocouples are just one example of an offset voltage source with temperature dependence. Another common source of offset voltage and offset drift results from input bias currents, namely input offset currents or differential input currents, when the input bias currents of a differential input pair are mismatched. An offset voltage forms when the differential bias current flows through any input-attached impedance, such as an input filter. The offset voltage will be proportional to the current and impedance, and both of these parameters (current and impedance) will typically have temperature dependence.

Additionally, offset and offset drift-like behaviors have been shown (reference) to result from solder flux residues remaining from the PCB assembly process. There, residues create parasitic conduction paths within the circuit and result in unpredictable behavior.

4 Block Diagram and Architecture

The block diagram of the AFE is depicted in Figure 8. The noisy 5-V supply is sub-regulated by the LDO regulator LP5907, which generates the 3.3-V supply voltage. The resistive strain gage bridges are supplied through PMOS CSD23381F4 and NMOS CSD13381F4 transistors. The same excitation voltage becomes after filtering the ratiometric reference for the delta-sigma DS ADC ADS1220. The outputs of the strain gage bridges respectively load cells are connected either hardwired or through TS5A21366 switches to the input filter and analog inputs of the ADS1220. The microcontroller MSP430G2553 controls the bridge excitation, switch configuration, the operation of the ADC, interfaces with the main controller and optional remote TMP01 digital temperature sensors, and drives the LED indicators. The TPD4E1U06 protects the AFE interface to the strain gage bridges against electrostatic-discharge (ESD) damage.

Copyright © 2016, Texas Instruments Incorporated
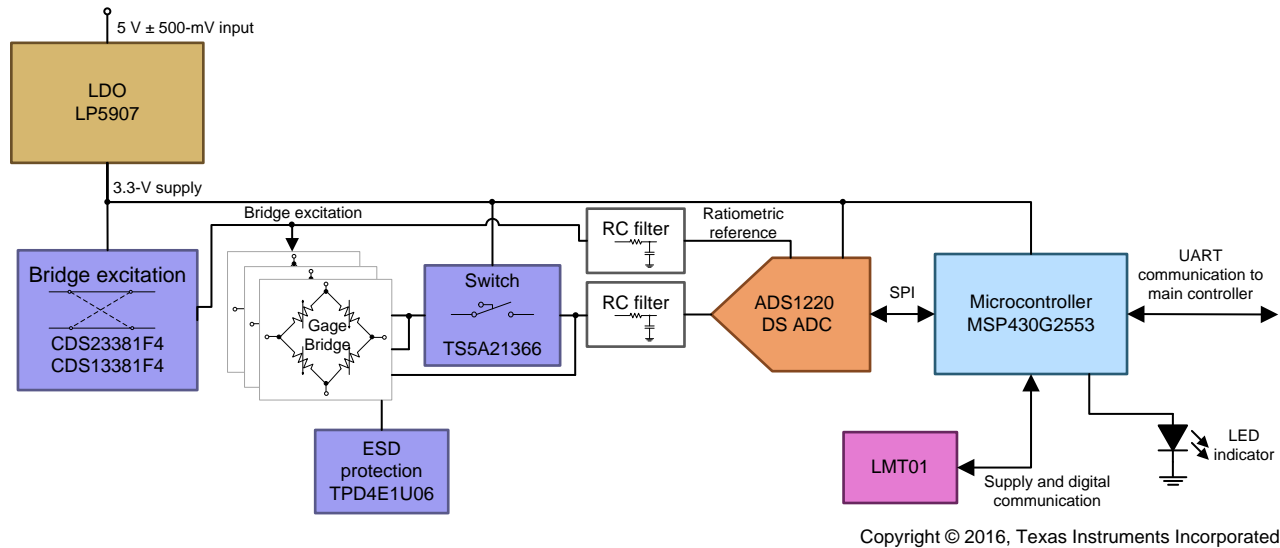
Figure 8. Block Diagram

4.1 Active Component Selection and Configuration

The 5-ppm Front-End for Weight and Vibration Measurement TI Design includes the following devices:

- ADS1220: Low-noise, 24-bit, single-cycle-settling, low-power ADC for small signal sensors
- LP5907 250-mA, ultra-low noise low-dropout regulator with excellent high-frequency power supply rejection ratio in face of high-load currents
- MSP430G2553: 16-bit mixed signal microcontroller
- TS5A21366: Low-leakage, 0.75-Ω dual analog switch with input logic
- TPD4E1U06: Quad-channel High-speed ESD protection device
- CSD23381F4: 12-V , P-channel FemtoFET™ MOSFET
- CSD13381F4: 12-V, N-channel FemtoFET MOSFET
- LMT01: 0.5°C accurate 2-pin temperature sensor with a pulse train interface

For more information on each of these devices, see their respective product folders at www.ti.com.

4.1.1 ADS1220

The ADC performance usually determines the system performance of most measurement systems and is consequently identified first. As performance needs of the weight measurement mode are more stringent, the following refers to the weighing mode unless stated otherwise. The theoretical maximum number of counts and minimum resolution is determined in Equation 6 as the quotient of the full-scale load divided by the desired scale weight resolution.

$$\left(\text{Max counts} \right) = \frac{\left(\text{Max load} \right)}{\left(\text{Weight resolution} \right)} = 15{,}000 \sim \log_2 \left(15{,}000 \right) = 13.9 \text{ bits}$$

(6)

Practically, the resolution needs to be at least 2 bits higher to keep the contributions of the quantization noise negligible versus other, harder to contain noise contributions. Moreover, an ADC of an even higher resolution is needed to account for dynamic range losses that occur when the input signal is not scaled (level shifted and amplified) to match the ADC's input range.

Therefore, the electrical resolution requirement for noise is more meaningful. It is determined by the product of the sensitivity times the target weight resolution divided by a margin factor to ensure stable readings in Equation 7. An overall sensitivity of 1 mV/kg times and 1-gram resolution with a safety margin of two translates into the requirement that the measurement system must be able to accurately resolve signals of at least 500 nV. So the electrical noise to be below 0.5 μV_{PP}. A 24-bit delta-sigma ADC is usually selected for this type of application.

$$\text{Noise}_{PP} = \frac{\text{Sensitivity} \times \left(\text{Weight resolution} \right)}{\text{Margin}} = \frac{1 \frac{\text{mV}}{\text{kg}} \times 1\text{g}}{2} = 0.5 \ \mu V_{PP}$$

(7)

The ADS1220, a 24-bit delta-sigma ADC, was chosen for its low-noise performance, integrated programmable gain amplifier (PGA), and single-cycle-settling decimation filter. The ADS1220 achieves both the critical resolution required for weight measurements and high sample rates for vibration measurements. Additionally, the ADS1220 provides internal multiplexers to switch the reference polarity for AC bridge excitation.

4.1.1.1 PGA Configuration

The ADS1220's integrated low-noise PGA provides gains up to 128 V/V. The highest gain setting that does not exceed the input voltage range requirements typically provides the best noise performance. The ADC's full-scale range scales with both reference voltage and gain. The full-scale range of the ADS1220 (as used in this design) is shown in Equation 8.

$$\text{FSR} = \frac{\pm V_{EXC}}{\text{Gain}} = \frac{3.3 \text{ V}}{128 \ \frac{\text{V}}{\text{V}}} = 25.8 \text{ mV}$$

(8)

In this design, the full-scale bridge output voltage is 15 mV; therefore, a gain of 128 V/V can be used. (See Table 9 in the ADS1220 datasheet (SBAS501).

4.1.1.2 Digital Filter Configuration

The FIR filter of the ADS1220 is highly configurable. For weight measurement, a data rate of 20 SPS in normal operation mode was chosen. This setting enables the activation of the integrated simultaneous 50/60Hz line cycle rejection filter option. At 20 SPS the ADS1220 resolution for a gain of 64 is mere 350 nV_{PP}, as shown by Table 1 in the section noise performance in the ADS1220 data sheet (SBAS501).

Alternative ADCs include:

* ADS1231: 24-bit with maximum sample rate of 80 SPS in case vibration detection is not required
* ADS1248: Higher precision 24-bit ADC with integrated 48-nV PGA and integrated MUX

4.1.2   LP5907

The LP5907 low-noise regulator is used in this design to sub-regulate a noisy 5-V output voltage of a very noisy switching supply to 3.3 V. It was chosen for its excellent loaded high-frequency noise suppression. Moreover, its drive capability, output voltage, and noise performance make it an ideal sensor supply for this application.

The LP5907 is a linear regulator capable of supplying a 250-mA output current. Designed to meet the requirements of RF and analog circuits, the LP5907-Q1 provides low noise, high PSRR, low quiescent current, and low line or load transient response. Using new innovative design techniques, the LP5907-Q1 offers class-leading noise performance without a noise bypass capacitor and the ability for remote output capacitor placement. The remote capacitor feature can save board space by using the capacitor of the supplied part.

The device is designed to work with a 1-µF input and a 1-µF output ceramic capacitor (no separate noise bypass capacitor is required). This device is available with fixed output voltages from 1.2 to 4.5 V in 25-mV steps. Texas Instruments Sales can provide for specific voltage option needs [Citation from snvs798i]. An increase of the output voltage of the LP5907 above 3.3 V will increase the excitation voltage and further improve the system signal-to-noise ratio.

Copyright © 2016, Texas Instruments Incorporated

Figure 9. LP5907 Functional Block Diagram

Alternative linear regulators include:
*   LP2951-33: A fixed 3.3-V output LDO, which supports higher V_{IN} range and drives loads up to 100 mA.

4.1.3 TS5A21366

The TS5A21366 is a dual single-pole single-throw (SPST) 0.75-Ω analog switch used to short the bridge's output voltages in weight measurement mode. This switch was chosen for its low on-resistance and low on-state leakage. The on-resistance of the bridge switch is important to consider in this application. When the outputs of the bridges differ, then the compensating current will flow through the switch. Then a voltage divider with the output resistances of the bridges and the switch forms. As the switch resistance changes over temperature, so would the voltage divider ratio and the weight reading captured by the ADC. That is unless the switches are sufficiently low resistance versus the bridges to neglect this effect. Also, mismatching leakage currents could become critical, especially at high temperatures and can introduce temperature drift as well.
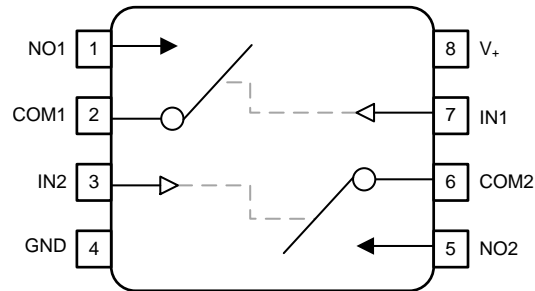
Copyright © 2016, Texas Instruments Incorporated

Figure 10. TS5A21366 Functional Block Diagram

Alternative switch for bridges with higher resistivity include:

- TS5A2066: Lower cost 10-Ω dual-channel SPST analog switch

16 *1-g Resolution Over 15-kg Range Sub-100-nV$_{PP}$ Noise Front-End Reference Design for Weight and Vibration Measurement*

TIDUBL0A–April 2016–Revised June 2016
Submit Documentation Feedback

4.1.4   MSP430G2553

The TI MSP430™ family of ultra-low-power microcontrollers consists of several devices featuring different sets of peripherals targeted for various applications. Combined with five low-power modes, the architecture is optimized to achieve extended battery life in portable measurement applications. The device features a powerful 16-bit RISC CPU, 16-bit registers, and constant generators that contribute to maximum code efficiency.

The digitally controlled oscillator (DCO) allows wake-up from low-power modes to active mode in less than 1 µs. The MSP430G2553 is an ultra-low-power mixed signal microcontroller with built-in 16-bit timers, up to 24 I/O capacitive-touch enabled pins, a versatile analog comparator, and built-in communication capability using the universal serial communication interface. In addition, the MSP430G2553 has a 10-bit ADC.

Typical applications include low-cost sensor systems that capture analog signals, convert them to digital values, and then process the data for display or for transmission to a host system (SLAS735).
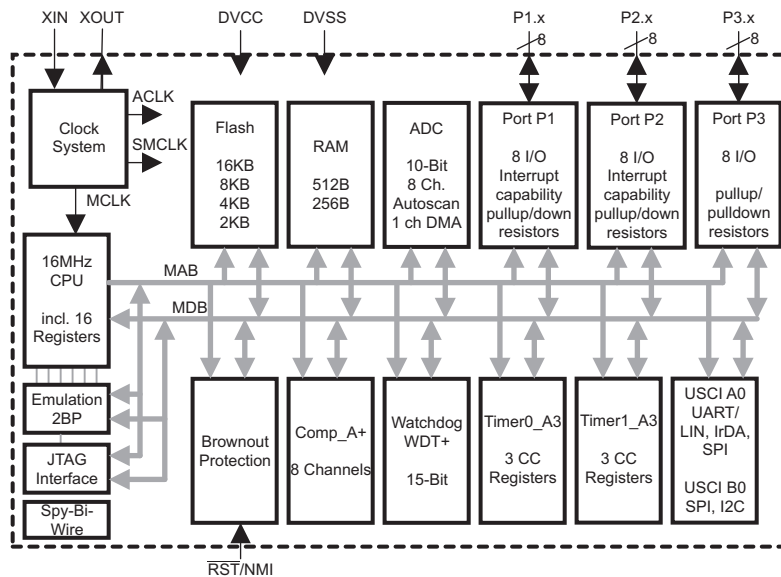
Copyright © 2016, Texas Instruments Incorporated

Figure 11. MSP430G2553 Functional Block Diagram

4.1.5 TPD4E1U06

The TPD4E1U06 is a quad-channel, low-leakage, unidirectional transient voltage suppressor (TVS) based ESD protection diode with ultra-low capacitance. This device can dissipate ESD strikes above the maximum level specified by the IEC 61000-4-2 international standard. It was chosen for its ultra-low leakage current of 1 nA (typ) and 10 nA (max).Though the leakage currents can be assumed to match well and cancel each other at first order, higher leakage currents could introduce a temperature drift at high temperatures and are consequently not desirable. Its 0.8-pF line capacitance makes it suitable for a wide range of applications (SLVSBQ9).

$$\Delta V_{ESDleakage}\left(85°C\right) \le I_{leakage(max)} \times Mismatch_{leakage} \times R_{BRIDGE} = 10\ nA \times 5\% \times 350\ \Omega = 60\ nV \tag{9}$$
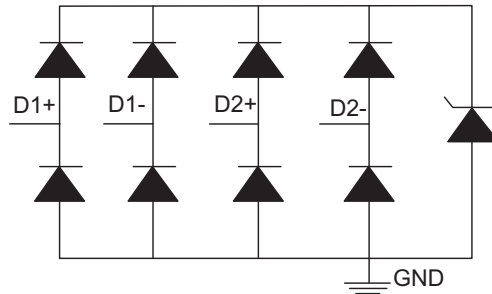
Copyright © 2016, Texas Instruments Incorporated

Figure 12. TPD4E1U06 Block Diagram

4.1.6 CSD23381F4 and CSD13381F4

This 150-mΩ, 12-V P-channel and 140-mΩ, 12-V N-channel FemtoFET MOSFETs control the bridge's excitation voltage polarity (for AC bridge excitation). These transistors were chosen for their low on-resistance, high peak currents, and their small form factor. The on-resistance of the bridge switch is important to consider in this application because a significant current flows through the bridge. In static operation, it is below 30 mA, but the dynamic current peaks after switching the polarity of the bridges AC excitation are much higher if decoupling capacitors are connected to the bridge supplies. The transistors are rated for peak currents up to 9 A and 7 A, respectively, which provides very robust margins for this application.
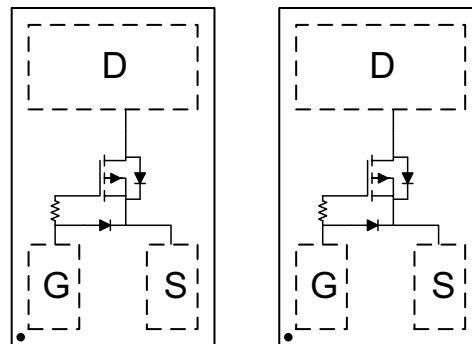
Copyright © 2016, Texas Instruments Incorporated

Figure 13. CSD23381F4 and CSD13381F4 Block Diagrams

Alternative parts for a bridge supply include:
- TS5A21366: 0.75-Ω, break-before-make dual analog switch with input logic

18 *1-g Resolution Over 15-kg Range Sub-100-nV$_{PP}$ Noise Front-End Reference Design for Weight and Vibration Measurement*

TIDUBL0A−April 2016−Revised June 2016
Submit Documentation Feedback

4.1.7 LMT01

Integrating the LMT01 as a wired temperature sensor enables the digital readout of remote temperature sensors and digital correct for temperature drift in case the bridges are exposed to different temperatures versus the AFE. If there is no such temperature difference, then the integrated temperature sensor of the ADS1220 could be used as well. The LMT01 is a high-accuracy, 2-pin temperature sensor with an easy-to-use pulse count interface, which makes it an ideal digital replacement for PTC or NTC thermistors both on and off board. The LMT01 digital pulse count output and high accuracy over a wide temperature range allow the device to pair with any MCU. TI's LMT01 achieves a flat ±0.5°C accuracy with very fine resolution (0.0625°C) over a wide temperature range of –20°C to 90°C without system calibration or hardware or software compensation.

Unlike other digital IC temperature sensors, the LMT01's single-wire interface is designed to directly interface with a GPIO or comparator input, thereby simplifying hardware implementation. Similarly, the LMT01's integrated EMI suppression and simple 2-pin architecture make it ideal for onboard and off-board temperature sensing. The LMT01 offers all the simplicity of analog NTC or PTC thermistors with the added benefits of a digital interface, wide specified performance, EMI immunity, and minimum processor resources (TIDUAU2).
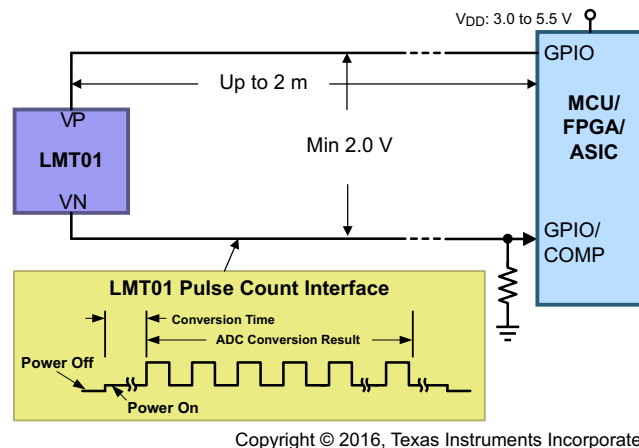
Copyright © 2016, Texas Instruments Incorporated

Figure 14. LMT01 Simplified Schematic

4.2 Signal Path Overview

In the beginning of this section, the block diagram introduced a general overview of the system functionality and the most suitable parts. This section discusses the analog signal path in more detail. The LP5907 regulator, depicted in the lower left of Figure 15, sub-regulates the noisy 5-V supply and provides a clean 3.3-V supply voltage to the AFE. The strain gauge load cell bridges are supplied through the PMOS CSD23381F4 and NMOS CSD13381F4 transistors featured in Figure 15. Alternating EXCA and EXCB are shorted to the 3.3-V low-noise supply voltage or the ground potential and so the supply polarity of the bridges is reversed to implement AC excitation. Excessive cross currents are avoided by a break-before-make sequence of the control signals CEXCAq, CEXCA, CEXCBq, and CEXCB, which are controlled by the MSP430G2553.
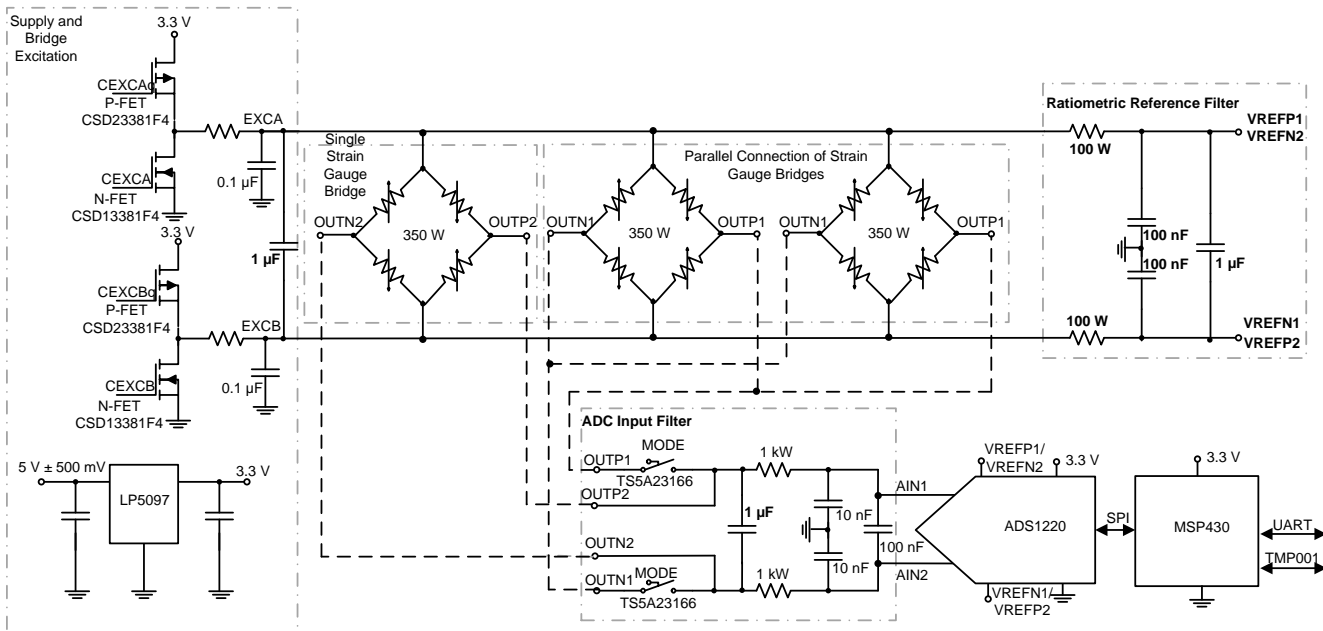
Copyright © 2016, Texas Instruments Incorporated

Figure 15. High-Level Circuit Concept of Weighing Scale AFE

The excitation voltage EXCA and EXCB are filtered with an RC filter. The filtered EXCA is connected to the VREFP1 and VERFN2 inputs to the ADS1220. Similarly, EXCB is connected to the VREFN1 and VERFP2 inputs to the ADS1220. Consequently, the internal multiplexer of the ADS1220 can be used to reverse the polarity of its reference when the polarity of the excitation is reversed. An external multiplexer is not required.

One pair of bridge outputs, OUTP2 and OUTN2, is hardwired to the input filter and analog inputs of the ADS1220. The outputs of the same polarity of the other bridges are shorted by the nets OUTP1 and OUTN1. OUTP1 and OUTN1 can be connected through the TS5A21366 switches to the input filter and analog inputs of the ADS1220. In weight measurement mode, the switches are closed and all bridge outputs of the same polarity are shorted. In this configuration, the voltage across the ADC inputs AIN1 and AIN2 becomes the average of the individual bridge output voltages. In vibration measurement mode, the switches are open and only the hardwired outputs OUTP2 and OUTN2 are connected to the ADC inputs AIN1 and AIN2, respectively. In this configuration, the ADC captures only the one individual bridge output.

Besides controlling bridge excitation, switch configuration, and ADC operation, the microcontroller calculates the sliding average before sending the conversion result to the main controller.

4.3   Filtering and Passive Component Selection

To achieve the desired noise performance, filtering is an important aspect to maintain signal integrity. The trade-off to consider is between lowest cutoff frequency to suppress high frequent noise, timely settling of signal after polarity reversal, and avoidance of introduction of offset drift due to the effect of voltage drop across filter resistors due to mismatching leakage currents. As a tradeoff, a differential mode 3-dB cutoff frequency of 689 Hz and a common mode 3-dB cutoff frequency of 14.5 kHz was chosen, which gives the absolute minimum of 25-dB damping at the delta-sigma modulator frequency of 256 kHz. Find more details in the ADS1220 application report (SBAA201). Moreover, alternatively using matched C2Y capacitors enables more attenuation and much better high-frequency noise rejection, which is described in detail in the TIPD188 design guide (TIDUAC1).

4.4   Test Circuitry

The central performance characteristics of the AFE are noise and drift. A simple test circuitry can easily evaluate these performance parameters of the AFE robustly and independently of other factors or costly equipment.

Two resistive test bridges are implemented on the TIDA-00765, which can be connected by wires to the AFE. They consist as depicted in Figure 16 of unbalanced bridges build-up from constant low temperature coefficient resistors. These constant resistor test bridges are insensitive towards mechanical vibrations and enable an accurate AFE performance test. Switches enable the simulation of load changes. Dependent of the position of DIP switches, the test bridges emulate the symmetric output signal changes between fully and half loaded load cell strain gauge bridges in terms of voltage level and output resistance. The left test bridge emulates a single resistive strain gauge load cell while the right bridge emulates the parallel connection of multiple gauges.
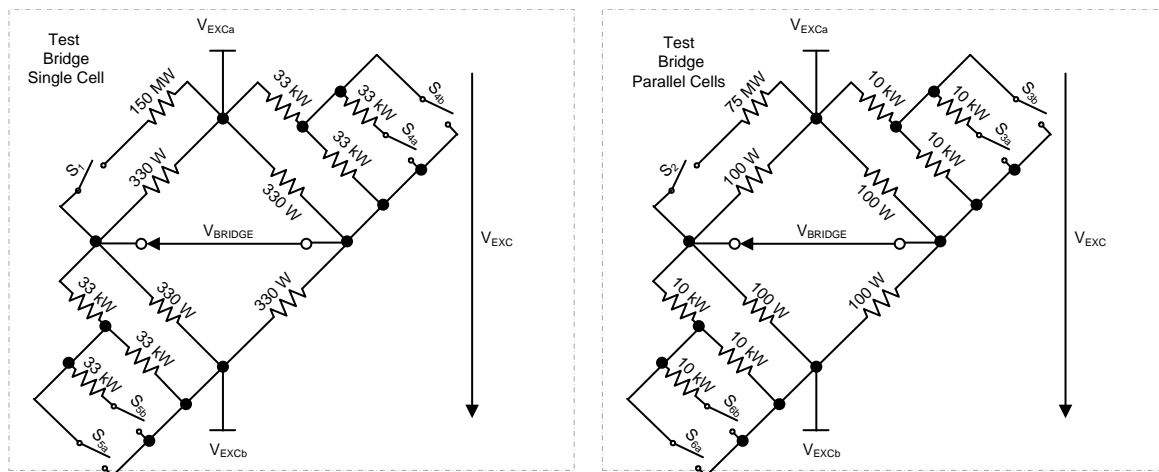
Figure 16. Test Bridge Schematics

The main resistor values were chosen for their low temperature drift and accuracy. Due to the resistances and small currents switched, the influence of the switches is non-negligible. This is especially true for the small signal switches S1 and S2. To minimize influence on the test bridge's temperature drift on the temperature characterization of the AFE, these test bridges can separate from the AFE and so be kept outside the temperature chamber during temperature sweeps testing the influence of temperature on the offset and noise of the AFE.

Table 6 provides an overview of the switch configurations and calculated output voltages.

Table 6. Overview of Test Bridge Output Voltages Calculated From Resistance Values of Schematics

SWITCH POSITIONS		TEST BRIDGE SINGLE CELL	TEST BRIDGE PARALLEL CELLS
(S1 = OPEN AND S2 = OPEN)		**(V$_{BRIDGE}$)**	
S3b=S4b=S5a=S6a=Open	S3a=S4a=S5b=S6b=Open	8.229 mV	8.229 mV
S3b=S4b=S5a=S6a=Closed	S3a=S4a=S5b=S6b=Open	10.96 mV	10.96 mV
S3b=S4b=S5a=S6a=X	S3a=S4a=S5b=S6b=Closed	16.42 mV	16.42 mV

5   Getting Started Hardware

To operate and reprogram the TIDA-00765, use the following:

- A TIDA-00765 circuit board
- A Spy-Bi-Wire™ interface as the MSP430 USB Debugging Interface or MSP430G2553 LaunchPad™ to program the controller
- A UART Interface capable of a baud rate of 115200 as the TTL-232R-3V3 USB-to-serial adapter cable to read out data
- Six female-to-female wire jumpers
- A 5-V power supply with cables

Figure 17 shows the overview of the TIDA-00765 circuit board. On the left part of the board are the MSP430G2553, ADS1220, and other components of the AFE. On the left side of the AFE is the UART interface J10. On top are the connectors to the optional LMT01 J9 and the Spy-Bi-Wire interface J12 from left to right. In the upper right corner of the AFE are the two alternative supply connectors, J5 and J6. The connector for the single gauge is located in the middle of the left edge of the AFE. The connector for the other gauges is located below in the lower left edge of the AFE. Two test bridges that emulate several strain gauges are located left of the AFE on left side of the board.
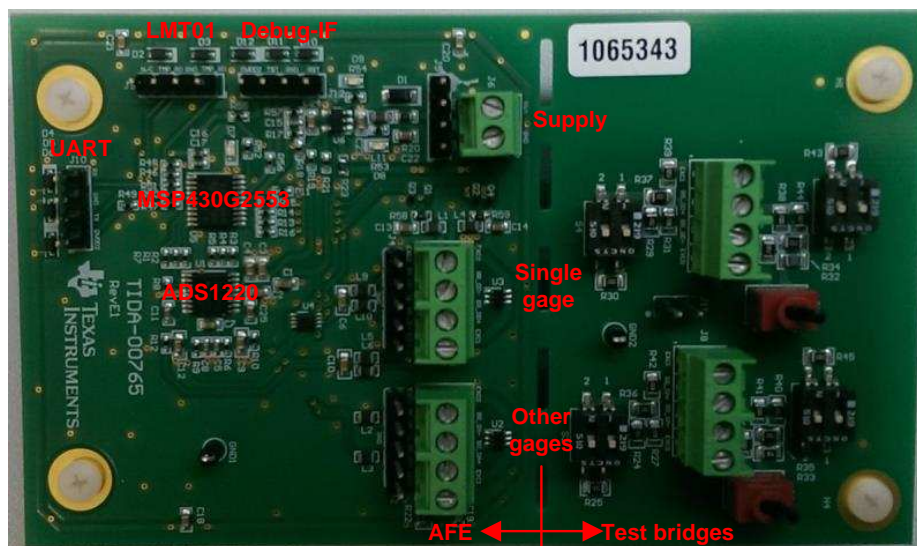
Figure 17. Board Overview Connectors

To measure weight, connect external strain gauges through J3 (single gauge) and J1 (other gauges). Alternatively use connectors J4 and J2 instead of J3 and J1.

To test TIDA-00765 functionality, connect test bridges to the ADS1220 by connecting J3 with J7 and J1 with J8. Use the switches S4 and S5 or S3 and S6 to vary the differential offset signal at the input of the ADS1220 between 8 to 20 mV. The switches S1 to S2 can be used to emulate small signal changes if the load they are switching is much smaller than their isolation resistance.

To connect and power up the TIDA-00765 and LaunchPad:

1. Download and install the newest Code Composer Studio™ (this test uses 6.1.1.00022): http://processors.wiki.ti.com/index.php/Download_CCS

2. Remove all jumpers on J3 of the MSP430G2553 LaunchPad.

3. Connect RST, Test, and GND from J12 of the TIDA-00765 to RST, Test (left side of J3) and GND (J2 or J6) of the MSP430G2553 LaunchPad, respectively.
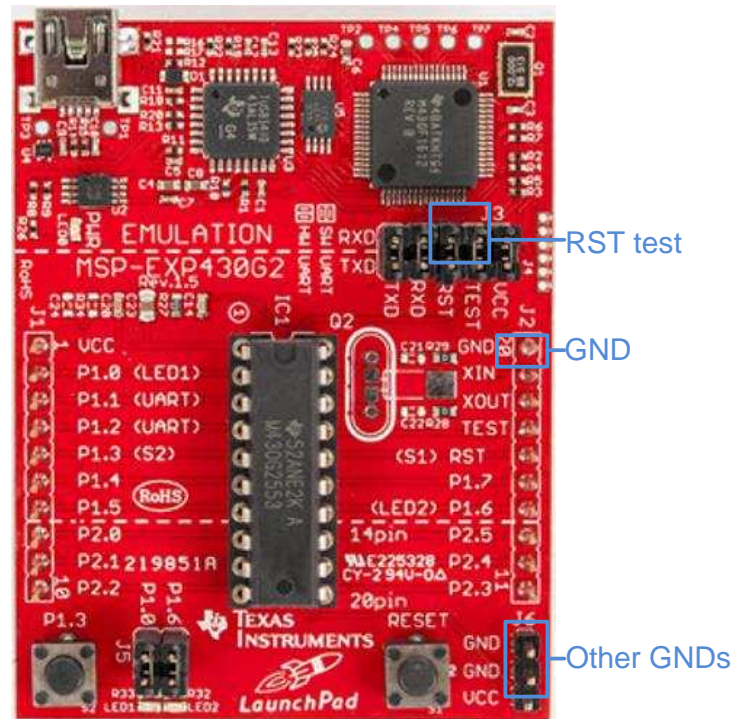
Figure 18. Overview of LaunchPad and Connectors

4. Connect TX, RX, and GND from J10 of the TIDA-00765 to TX, RX, and GND (yellow, orange, and black) of the TTL-232R-3V3 cable, respectively.

5. Connect the TIDA-00765 through J5 or J6 to the power supply and apply 5 V.

6. Connect the MSP430G2553 LaunchPad USB port to the computer.

7. Connect the TTL-232R-3V3 cable to the computer.

To reprogram the MSP430G2553:

1. Open CCS.
2. Select your workspace (default click on OK).
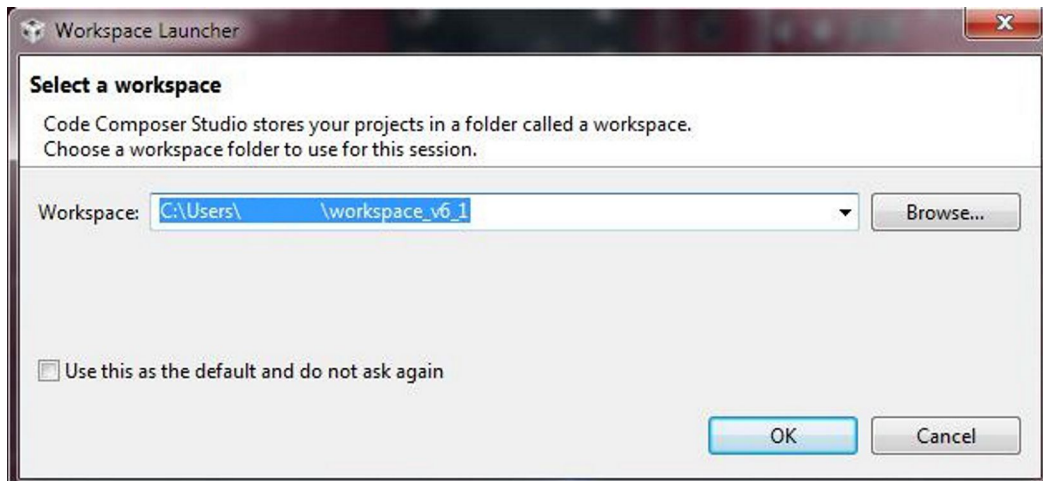
Figure 19. Selecting Workspace

3. Click on CCS Edit in the upper right corner.
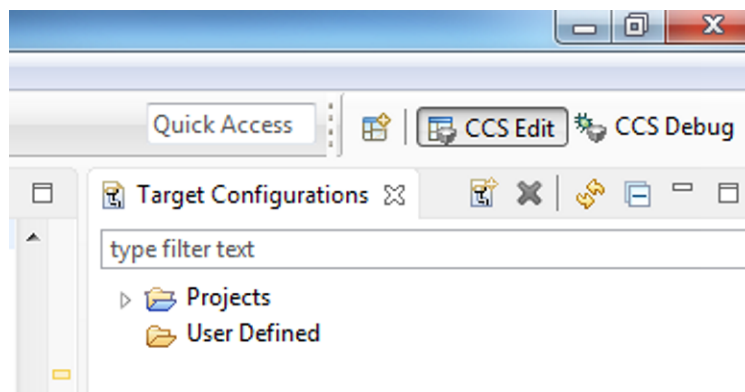
Figure 20. Selecting Edit Mode

4. Click on Project → Import CCS Project and choose the folder with the unzipped TIDA-00765 firmware.
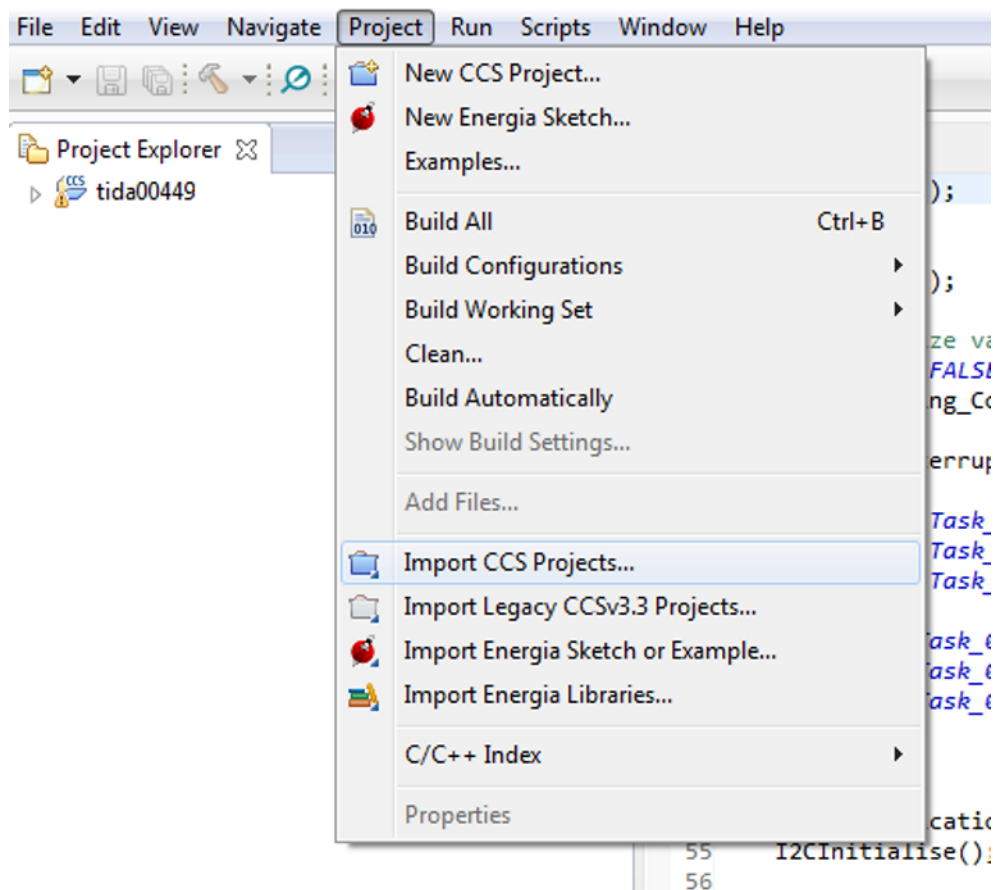
Figure 21. Import CCS Project

5. Click on the debug button in the upper left [button image].

6. If it succeeds, the MSP430G2553 is now programmed. If it failed, make sure that the MSP430G2553 is powered (see Steps 1 through 8) and that the connecting cables are correct (see Steps 4 and 5 under first-time users). Also, check whether the right device, the MSP430G2553, is loaded in the target configuration. CCS may not indicate a connection due to limitations of the USB emulator of the LaunchPad.

7. Click on the resume button in the upper left [button image].

8. The MSP430G2553 is now programmed and running. Verify by running the MSP430G2553 in debug mode and check for the advances of the firmware program execution.

9. A general serial communication monitor tool can be used to log the conversion data from the AFE, such as Comm Operator Pal from http://www.serialporttool.com/.

10. If necessary, click on File → Open Connection.

11. In the Serial Port Setting tab, select the appropriate port name for the TTL-232R-3V3. Set the baud rate to 115200 and leave the other fields as default. Then click OK. The communication should now be established.
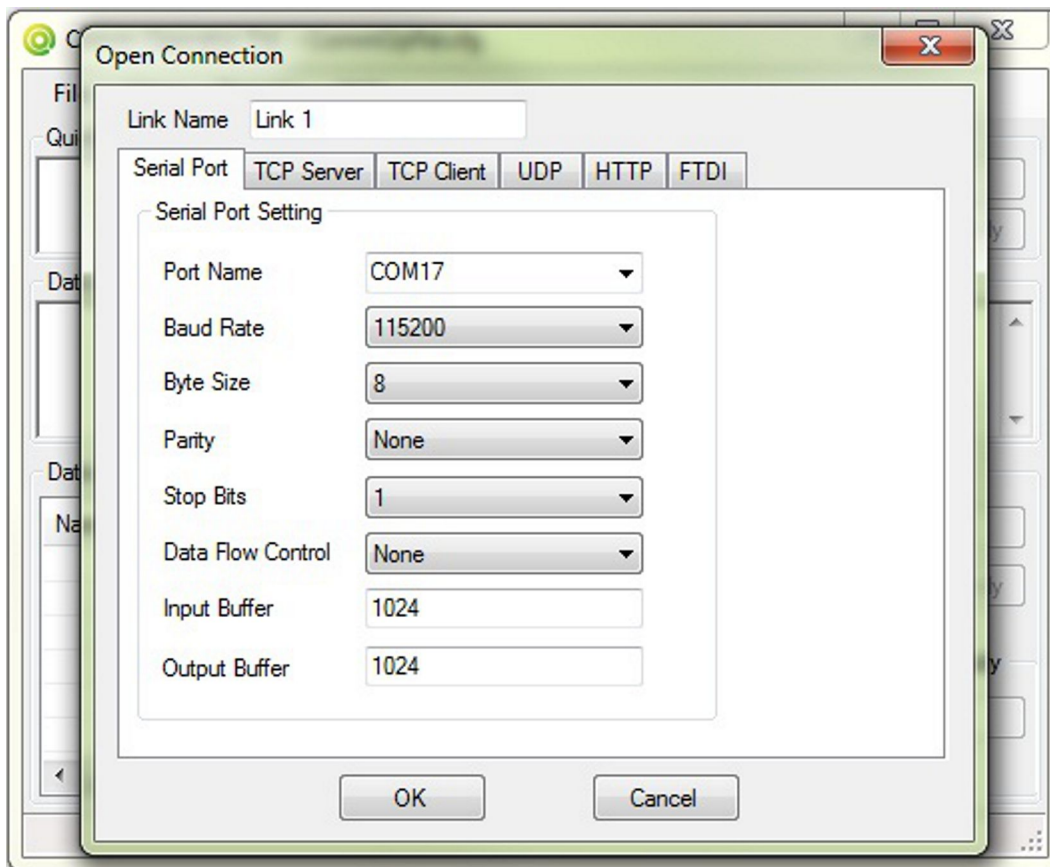
Figure 22. Communication Settings

12. Verify that the lines are incremented in the Comm Operator Pal – Data Log (Text) Window. If not, go through Steps 1 through 11.

13. To save the log file, click on File → Save Log in the Comm Operator Pal main window. After the sequence, log what occurred and save the data. (Clicking saves all the communication that is displayed in the tab.)

6 Getting Started Firmware

6.1 Overview

The TIDA-00765 firmware is based on the MSP430G2553 and communicates with the ADS1220 through GPIO-emulated SPI bus signals. The communication part of the firmware is based on the TIDA-00165 firmware with a mapping method that modifies the register bit field. The firmware can be configured to drive the measurement bridge excitation in either AC or DC mode with the fixed time flow described in Section 6.3, and keeps reading conversion results out from the onboard ADS1220 once valid data is ready (DRDY is valid). Conversion results are sent out through the UART port of the MCU to the host (for example, PC).

The firmware also provides driver module for the off-board digital temperature sensor LMT01 and is explained in Section 6.4.

6.2 Build Options

There are several build options provided in the header file drivers.h.

6.2.1 Select Measurement Mode

There are two measurement modes provided
- Weight measurement mode
- Vibration measurement mode

The differences between the two measure modes are listed in Table 7:

Table 7. Measure Modes Description

PARAMETER	WEIGHT MEASUREMENT MODE	VIBRATION MEASUREMENT MODE
Default excitation method	AC excitation	DC excitation
Bridge switch	ON (bridges shorted)	OFF (bridges separated)
ADS1220 operating mode	Normal	Turbo
ADS1220 data rate	20 SPS	2000 SPS

The settings for each measurement mode can be changed in the firmware according to different use cases. The settings shown in Table 7 are default values.

Measurement mode is selected by the `#define` `__VIBRATION__` macro. Comment out this macro definition in drivers.h (line 41) to enable weight measurement mode, or keep the statement to enable vibration measurement mode.

By default, the firmware is working in weight measurement mode.

6.2.2 Select Driver Options

There are several lower level driver options provided along with the firmware. These options can be turned on and off in drivers.h in the lines following line 47 by keeping or commenting out macro definitions:

- **#define** `__BIT_FIELD__`

  Select whether to configure the ADS1220 registers over parameter type or bit field type data structure. A bit field type data structure provides more flexibility and is easier to read, but may take more time to execute for the CPU.

- **#define** `SAMPLE_POINTS       1`

  Set samples for sliding average filter. The user may set the sample points of the filter by changing the value of `SAMPLE_POINTS`. The value is set to 1 by default to disable filtering. `SAMPLE_POINTS` is used by an internal variable of a type unsigned char; therefore, the value can be between 1 and 255 (do not set to 0). The larger the value, the more RAM is consumed.

- **#define** `__CALIBRATION__`

  Select whether offset calibration is used for the conversion result. Comment out to disable offset calibration.

- **#define** `__LPM__`

  Select whether the MCU enters LPM0 low power mode when idle. LPM0 mode is disabled by default.

- **#define** `__LMT01__`

  Select whether the reading function of the temperature sensor LMT01 is enabled in the firmware. The LMT01 driver is explained in 6.4. LMT01.

6.3 Conversion Flow for AC Excitation Mode

The firmware works in AC or DC excitation mode. This can be configured by the macro definition of **#define** `__AC_EXCITATION__` in the file drivers.h. By default, the firmware works in AC excitation mode.

The conversion timing sequence in AC excitation mode is shown in Figure 23.

In DC excitation mode, the firmware does not alter the excitation polarity and continuously captures the readings and converts the result with polarity 0 active.

The firmware processes the data reading of each sample with a moving average algorithm (FIR filter) shown in Equation 10.

$$SMA(x) = \frac{x_p + x_{p-1} + x_{p-2} \cdots + x_{p-n}}{n}$$

(10)

where

- n is the total sample points of the filter.
- x_p is the latest sampled value.

The user can set the sample points of the filter by changing the definition of `SAMPLE_POINTS` in drivers.h as described in Section 6.2.2. The value is set to 1 by default to disable filtering.
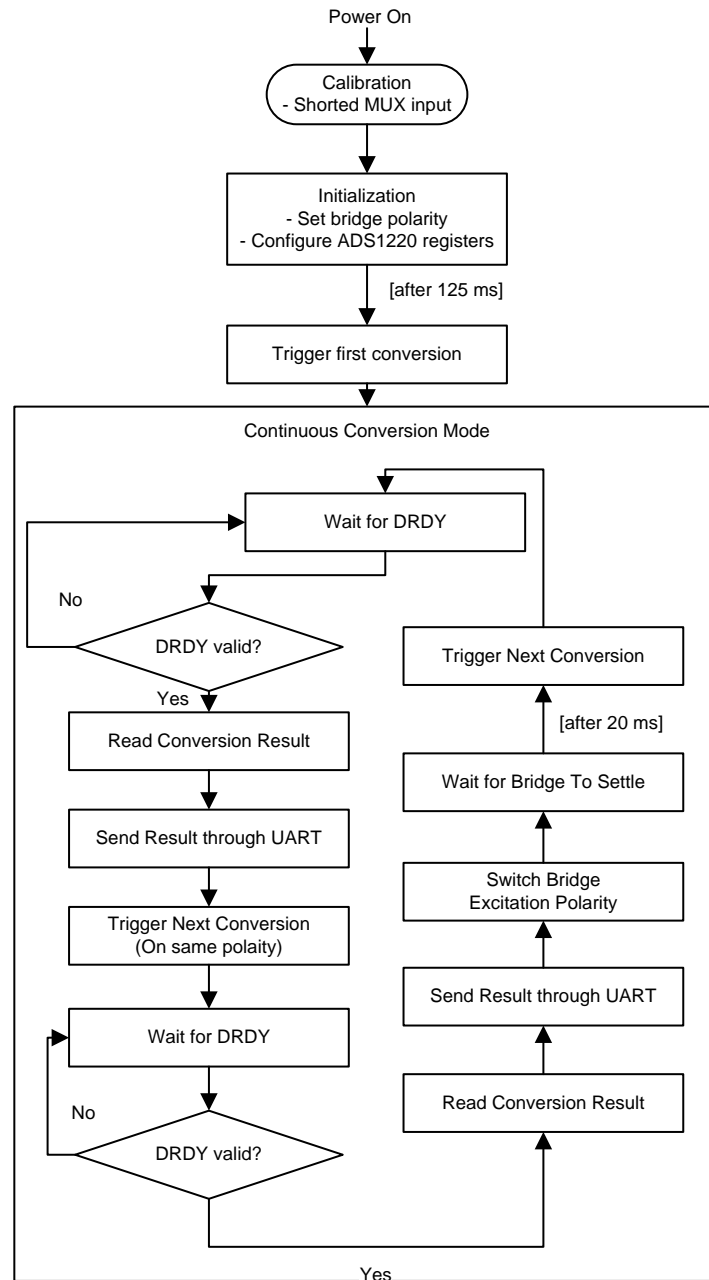
Figure 23. Flowchart of Conversion Timing

6.4 LMT01 Temperature Measurement

The LMT01 is a high-accuracy, 2-pin temperature sensor with an easy-to-use pulse count interface, which makes it an ideal digital replacement for PTC or NTC thermistors both on and off board in automotive, industrial, and consumer markets. Features like a pulse-counting based digital output and high accuracy over a wide temperature range allow the LMT01 to pair with any MCU without concern for integrated ADC quality or availability, while minimizing software overhead. TI's LMT01 achieves a flat ±0.5°C accuracy with a very fine resolution (0.0625°C) over a wide temperature range of −20°C to 90°C without system calibration or hardware or software compensation.

The sensor takes at max 51 ms to convert the temperature after powering up and 50 ms to transfer the data. This design checks the temperature of the LMT01 within a period of 1 second. In this design, the data sent by the LMT01 is captured by the analog comparator of the MSP430G2553. When setting the comparator threshold to 0.25 × V_{CC} (0.825 V), the high and low level output signal of the LMT01 has to be across the comparator threshold. Because the output current (IOL and IOH) of the LMT01 is in the range from 28 to 39 μA and 112.5 to 143 μA (respectively), a 10-kΩ resistor to ground is used, which generates 390 mV of VOL_max and 1.125 V of VOH_min. To power and read the LMT01 properly, a timing sequence is implemented in the firmware following the flowchart shown in Figure 24.
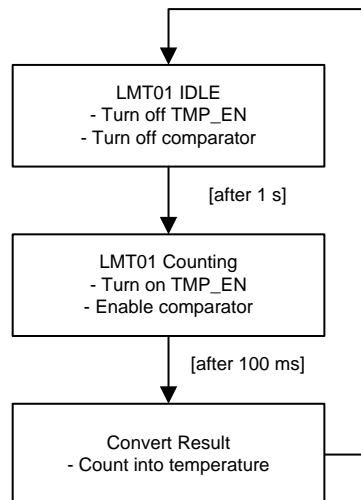
Figure 24. Flowchart of Temperature Conversion Timing

6.5 UART

A simple UART communication protocol is implemented between the TIDA-00765 and a host to collect the conversion results of the ADS1220.

Set the UART data format to the following:

- Baud rate: 115200 bps
- Parity: None
- Data bit: 8 bits
- Stop bit: 1 bit

The data transferred is in a format of decimal numbers in ASCII followed by a carriage return.

1-g Resolution Over 15-kg Range Sub-100-nV_{PP} Noise Front-End Reference Design for Weight and Vibration Measurement

7   Test Setup

7.1   Test Setup Based on Test Bridges

To evaluate the noise and drift performance of the AFE, two test bridges are foreseen on the TIDA-00765 circuit board. These test bridges do not exhibit sensitivity towards mechanical vibrations of resistive strain gauge load cells. This insensitivity helps quantify the performance of the AFE. For the following AFE performance tests, these test bridges are used. Cables from jumper J1 to J8 and J3 to J7 connect the AFE inputs to the outputs of test bridges and the AFE excitation with bridge supply rails. The specific test equipment used for these tests is listed in Table 8.

Table 8. Overview of Test Equipment Used

EQUIPMENT	TYPE	COMMENTS
Device under test	TIDA-00765 circuit board	
Power supply	Agilent 3631A	
Waveform generator	Keysight 33600A	
UART interface	TTL-232R-3V3 USB adaptor	
Spy-Bi-Wire interface	MSP430G2553 LaunchPad emulator	Disconnected for most tests after programming the 430
Temperature test chamber	Vötsch VT 4002	
Scope	Tektronix TDS2024B	

7.1.1 Measuring Over Temperature

The noise performance over temperature of the AFE are determined by measuring noise during a temperature sweep. As depicted in Figure 25, only the AFE was kept in the temperature chamber and shielded with a tissue from direct airflow of the ventilator. The AFE was connected through 1-m cables to the test bridge circuitry, which emulates the output signal of the fully or half-loaded load cell strain gauge bridge in terms of voltage level and output resistance. To minimize the test bridge drift, the test bridges are separated from the AFE and kept outside the temperature chamber in an airtight enclosure. The temperature sweeps from 25°C to 0°C and then up to 85°C, down to 0°C and back up to 25°C over the course of several hours. To properly settle the AFE and test bridge temperatures, both are monitored directly with attached temperature sensors. In retrospect, a non-air-tight enclosure like a tissue is better to shield the test bridges from turbulent airflows and keep the test bridges at a constant temperature.

The board was supplied by an Agilent 3631A power supply. The ADC conversion result data stream was captured with a TTL-232R-3V3 USB adaptor UART interface and a laptop.
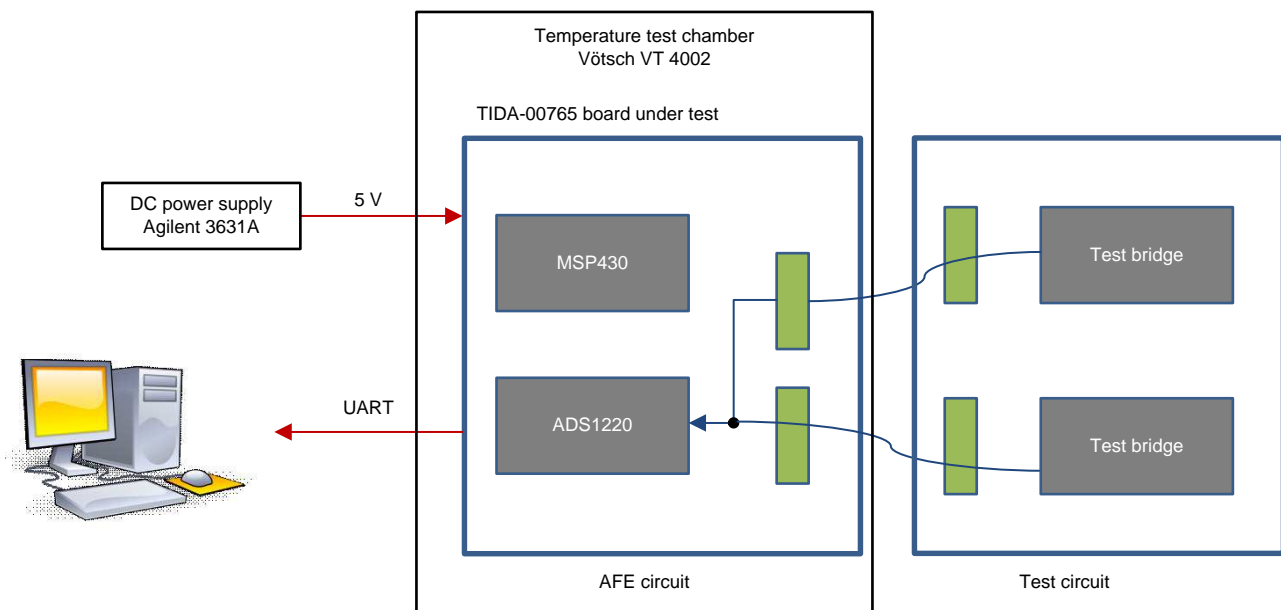
Copyright © 2016, Texas Instruments Incorporated

Figure 25. Diagram of Test Setup to Measure Noise Performance and Drift Over Temperature

7.1.2   Measuring Power Supply Rejection

Figure 26 shows the setup to test power supply rejection. A 100-kHz bandlimited noise is generated with a Keysight 33600A waveform generator. To overcome the generator's output range and load driving limitations, a 3-cell battery pack is used to add an offset to the output of the waveform generator, which was buffered and fed into the supply of the tested TIDA-00765 board by a BUF234 buffer. The buffer is powered from the Agilent 3631A power supply. The amplitude of the supply noise is recorded with an oscilloscope connected to the power supply of the TIDA-00765 board. The conversion data of the ADS1220 is captured again with the USB adaptor UART interface and a laptop.
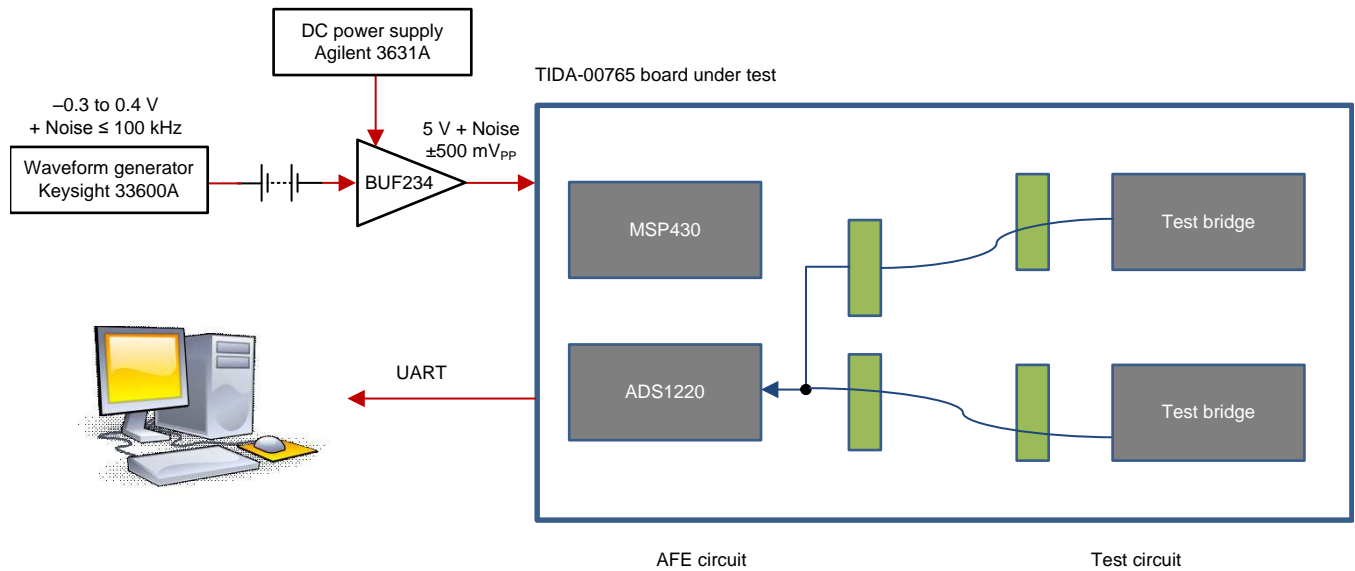
Copyright © 2016, Texas Instruments Incorporat

Figure 26. Diagram of Test Setup to Measure Supply Noise Rejection

Figure 27 shows the actual test setup for the measurement of supply noise rejection.
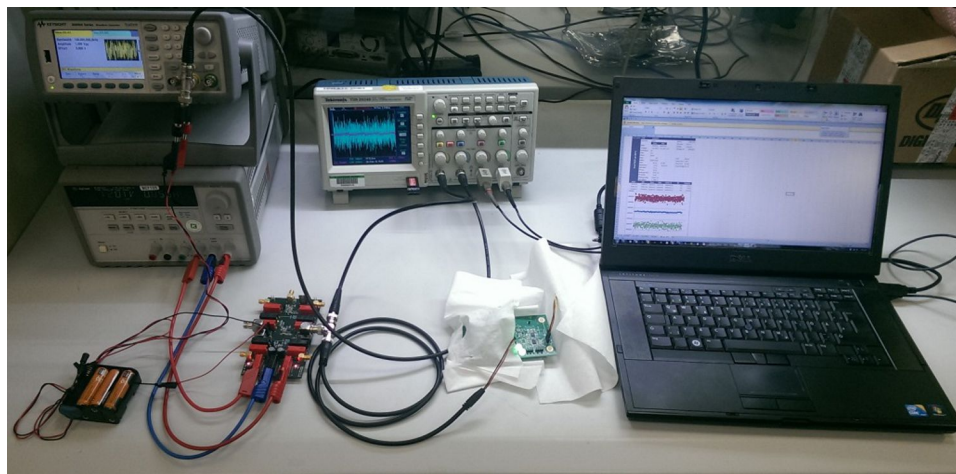
Figure 27. Picture of Test Setup to Measure Supply Noise Rejection

7.1.3 Measuring Robustness to Capacitive Noise Injection

To investigate the robustness of the AFE to capacitive coupled noise, for example of a switching power supply, such noise is generated by a Keysight 33600A waveform generator and injected asymmetrically into a single AFE analog input through ceramic capacitors (see Figure 28). The amplitude of the injected 100-kHz bandlimited noise is swept and correlated with the noise level of the ADC conversion results during the sweep to identify the sensitivity of the design. Again, the Agilent 3631A is the power supply and the data stream is captured with a TTL-232R-3V3 USB adaptor UART interface and a laptop.
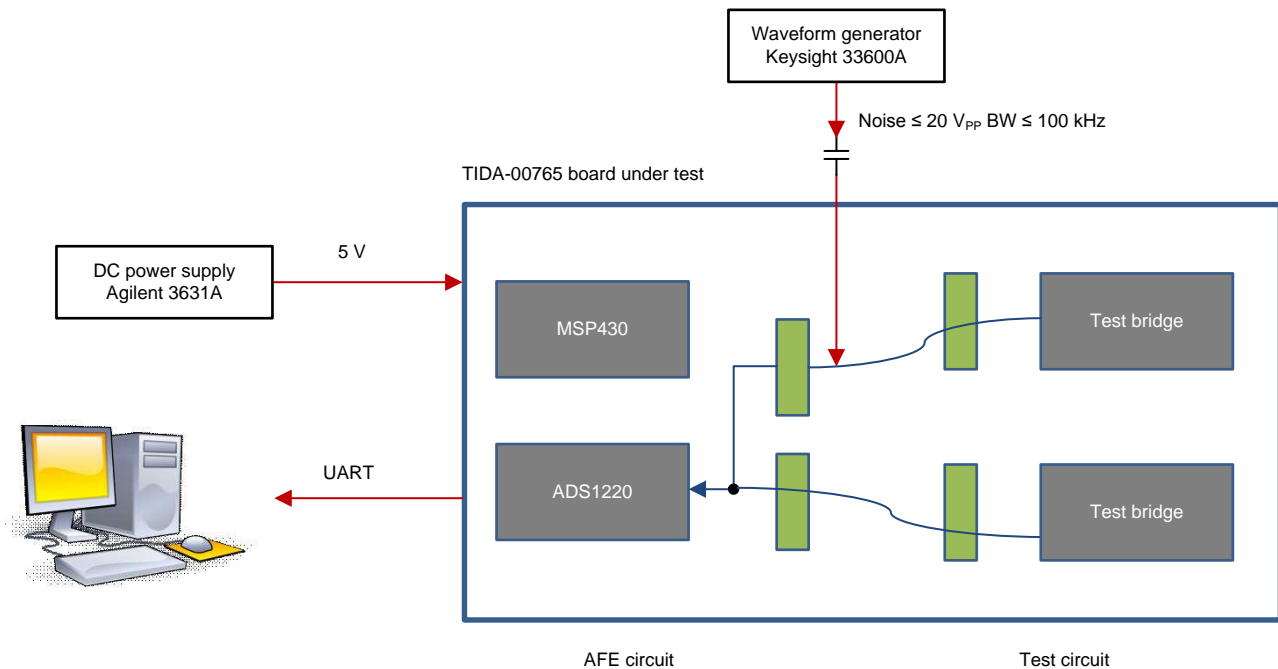
Copyright © 2016, Texas Instruments Incorporat

Figure 28. Diagram of Test Setup to Measure Supply Noise Rejection

TIDUBL0A−April 2016−Revised June 2016
Submit Documentation Feedback

1-g Resolution Over 15-kg Range Sub-100-nV$_{PP}$ Noise Front-End Reference Design for Weight and Vibration Measurement 35

7.2   Test Setup With Advanced Food Processor

To measure weight with the food processor, all three the weight scales are shorted together and connected to the TIDA-00765, the AFE input left and right feet are shorted to J3, the front foot is connected to J1, and both inputs are shorted with the TS5A21366 on the TIDA-00765 board (see Figure 29).

Copyright © 2016, Texas Instruments Incorporated
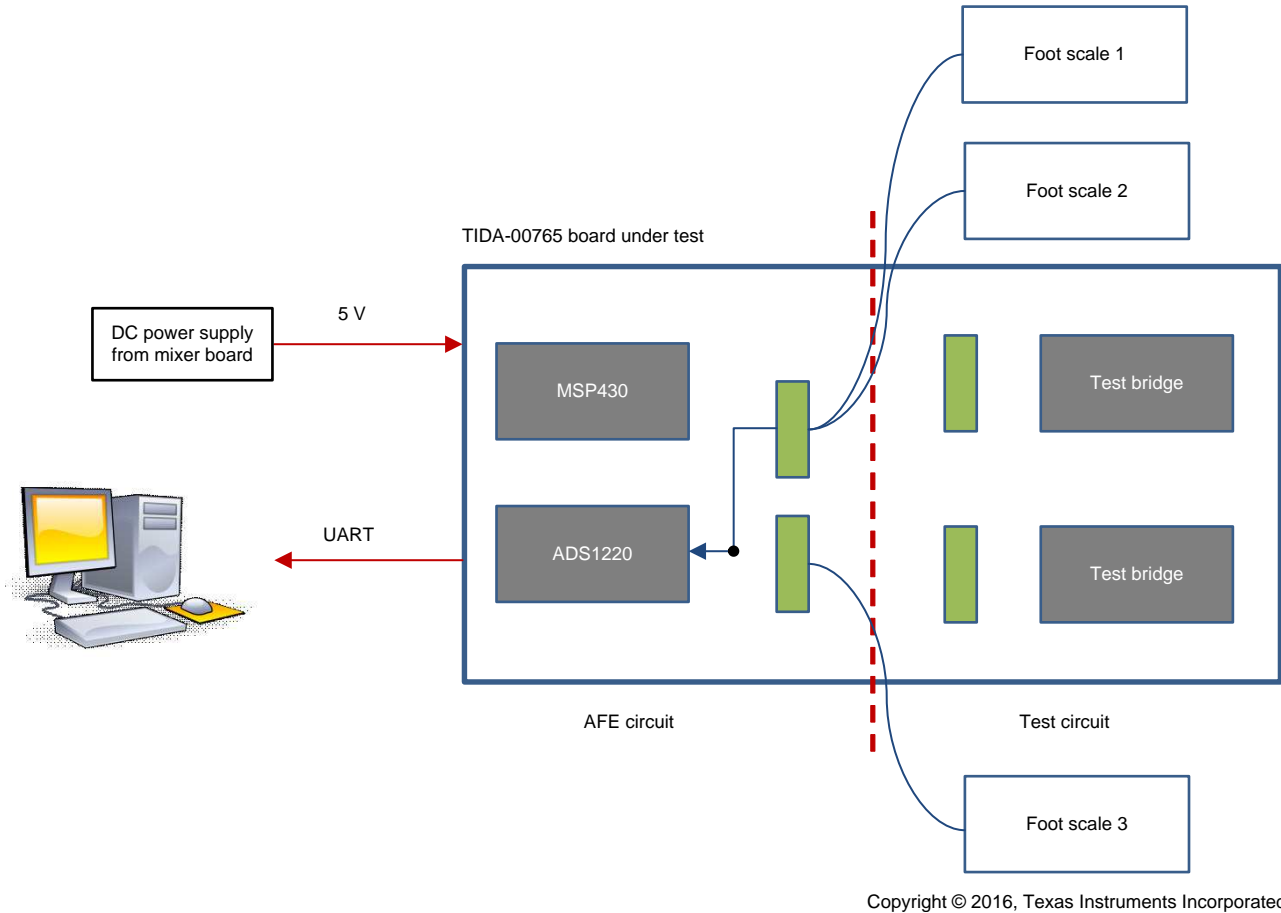
Figure 29. Diagram of Test Setup to Measure Weight With Food Processor Scales

To measure vibrations with the food processor, only the left weight scale is connected to J3 of the TIDA-00765 board as shown in Figure 30.

Copyright © 2016, Texas Instruments Incorporat
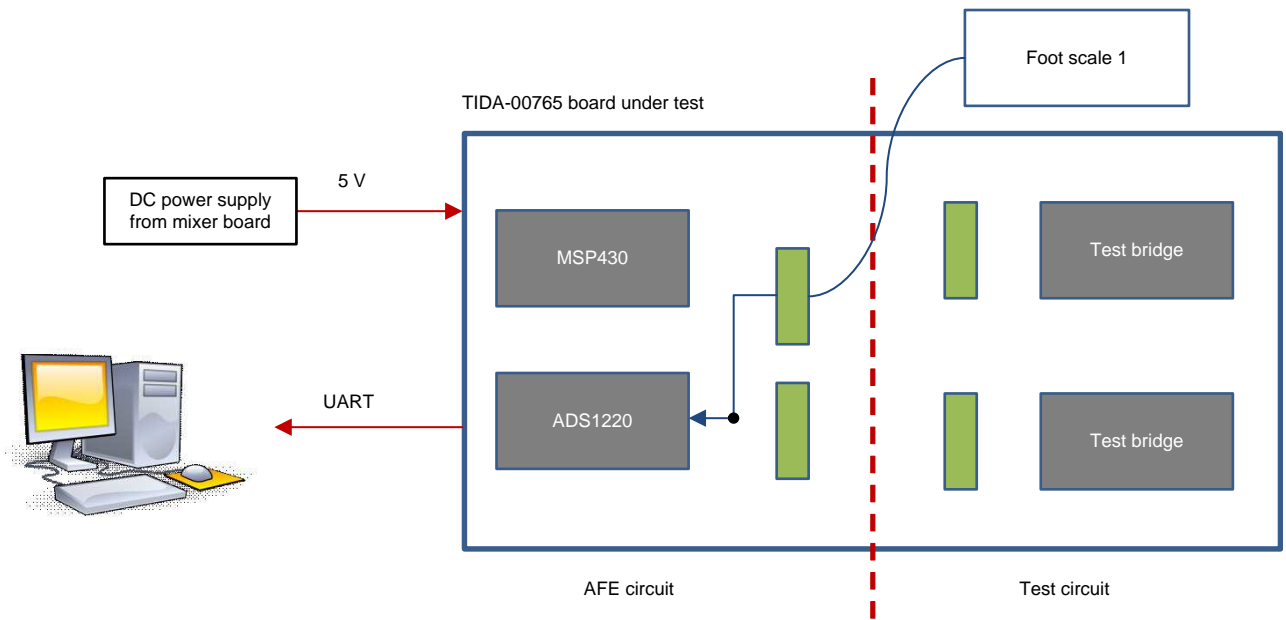
Figure 30. Diagram of Test Setup to Measure Vibrations With Food Processor Scales

8   Test Data

Low noise and temperature drift create an accurate weighing scale and a good user experience, both the critical parameters. Section 8.1 focuses on these parameters in the following performance tests of the AFE in weighing mode parameters. Then, Section 8.2 showcase the performance of an off-the-shelf advanced food processor for weight and vibration measurement.

8.1   *Tests With Integrated Test Bridges*

Integrated on this TI Design are resistive bridges to emulate the loaded strain gauge bridges. In the following tests, these test circuits generate the input signal for the AFE.

8.1.1   Noise Performance versus Temperature

The noise performance of the AFE is determined by measuring noise during a temperature sweep. Only the AFE is kept in the temperature chamber to focus on its performance over temperature. It was connected to a test bridge emulating fully loaded strain gauges. The temperature is swept from 25°C to 0°C, then up to 85°C, down to 0°C, and back up to 25°C. The result of this sweep is depicted in Figure 31. The peak-to-peak noise value of the raw data at 20 SPS and a gain of 64 is slightly above 40 µV. The RMS noise of the raw data is below 15 µV. The sliding average reduces the peak-to-peak value to below 0.06 μV_{PP}. This value is almost an order of magnitude below the maximum limit for the filtered readings of 0.5 μV_{PP}. This significant margin either guarantees a very stable display or enables using lower cost strain gauges with reduced sensitivity. Overall, the noise of the AFE is over temperature very well within specification.
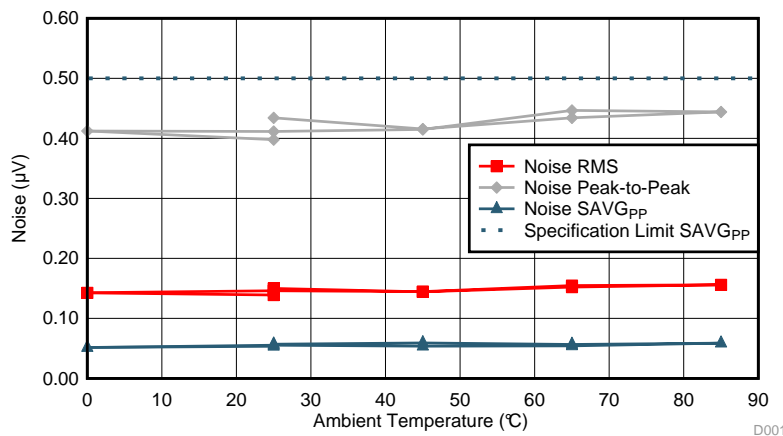
Figure 31. Noise Level of Raw Data With Sliding Average Filtered Data as RMS Value and Peak-to-Peak Value Within 1 Second

38   *1-g Resolution Over 15-kg Range Sub-100-nV_{PP} Noise Front-End Reference Design for Weight and Vibration Measurement*

TIDUBL0A – April 2016 – Revised June 2016
Submit Documentation Feedback

8.1.2 Robustness versus Supply Noise

The AFE is integrated into a harsh environment and exposed to high levels of switching noise. To quantify the robustness versus supply noise, 500-mV$_{PP}$, 100-kHz bandlimited noise is injected into the AFE supply at the Vin connector. The injected noise and the reduction of the noise through the excellent sub-regulation by LDO can be seen in Figure 32 a). The noise level in this test case is a worst case scenario, versus the actual noise in a real mixer, which is depicted in Figure 32 b). With the noise injection of 500 mV$_{PP}$, no increase in noise level of the readings is observable. Additionally, the supply voltage and the headroom of the LDO are reduced to worsen the test conditions for the LDO and AFE further. The recorded noise level versus supply voltage of the AFE is depicted in Figure 32 c). As long as the headroom of the LDO is greater than 200 mV and the supply voltage above 3.5 V, the noise of the filtered readings is not impacted at all. This proves the LDO's excellent sub-regulation and outstanding robustness of the AFE to switching supply noise.
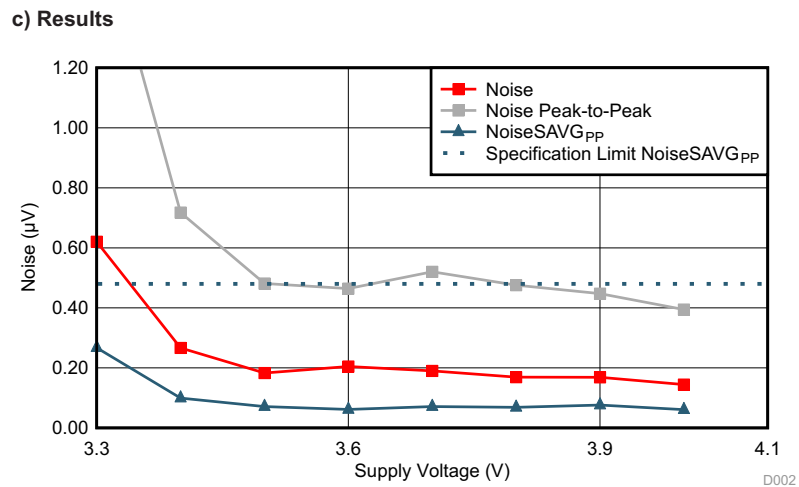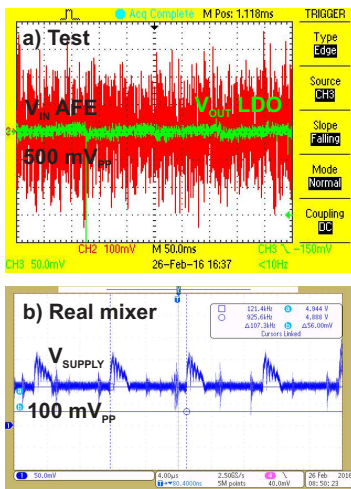
Figure 32. Noise Readings versus Heavy Supply Noise

TIDUBL0A–April 2016–Revised June 2016
Submit Documentation Feedback

1-g Resolution Over 15-kg Range Sub-100-nV$_{PP}$ Noise Front-End Reference Design for Weight and Vibration Measurement

39

8.1.3 Robustness versus Capacitive Coupled Noise

Section 8.1.2 tested whether switching noise could couple through the supply into the AFE. Unfortunately, this is not the only path in which disturbances can interfere with the noise performance of the AFE. Another mechanism can be the capacitive coupling, such as through the wires connecting the strain gauge bridges with AFE. The robustness versus capacitive coupled noise is quantified by injecting noise through a capacitor into a single AFE input at the bridge connector during data capture. The amplitude of the 100-kHz bandlimited noise was swept from 2 mV_{PP} to 20 mV_{PP}. A realistic coupling capacitance of 10 pF did not show any impact upon the noise performance up to noise amplitudes of 20 V_{PP} as Figure 33 shows. Consequently, the test is repeated with an unreasonably increased coupling capacitor of 1 nF. In this case, the noise amplitude did not observably increase the noise amplitude below 2 V_{PP}. This result proves that the AFE is highly robust to the harsh environment and disturbances of switching supplies.
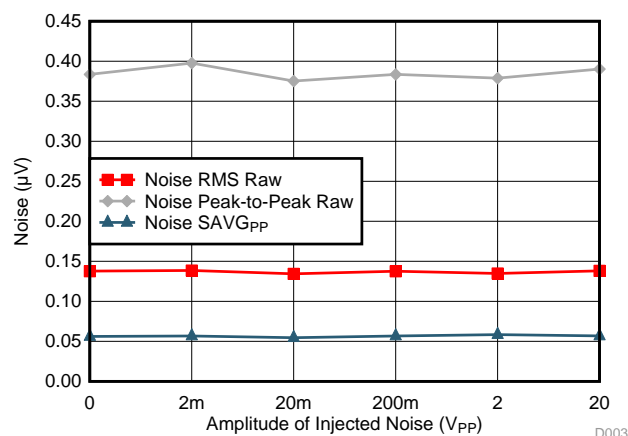
Figure 33. Noise Readings versus Heavy Supply Noise (Noise Coupling With C$_{COUPL}$ = 10 pF)
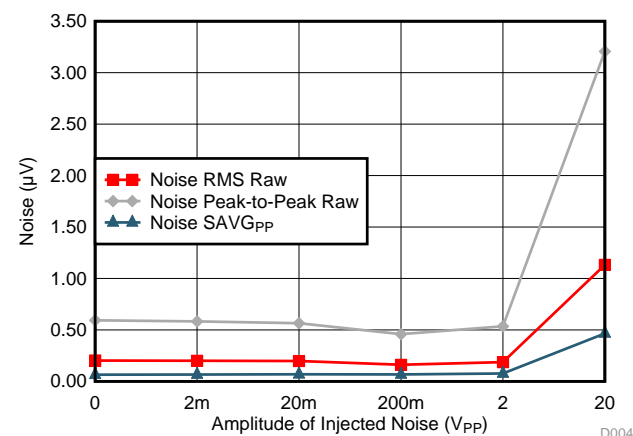
Figure 34. Noise Readings versus Heavy Supply Noise (Noise Coupling With C$_{COUPL}$ = 1 nF

40   *1-g Resolution Over 15-kg Range Sub-100-nV$_{PP}$ Noise Front-End Reference Design for Weight and Vibration Measurement*

TIDUBL0A−April 2016−Revised June 2016
Submit Documentation Feedback

8.1.4   Temperature Drift

Stable readings require a low temperature drift. To quantify the AFE temperature drift, the readings and their change are measured over a temperature sweep. Only the AFE was kept in the temperature chamber. The AFE is connected to a test bridge emulating fully loaded strain gauges. The test bridge is kept in a sealed plastic enclosure outside of the temperature chamber. The temperature was swept from 25°C to 0°C and then up to 85°C, down to 0°C and back up to 25°C. The change of the reading is depicted in Figure 35. The reading changes by less than 5 µV over the complete temperature range from 0°C to 85°C. According to the box method, the temperature drift of the AFE is therefore 0.05 µV/°C, which is significantly below the specification value of 10 µV/10°C. Moreover, the non-linear offset change is cancelled due to the AC excitation.
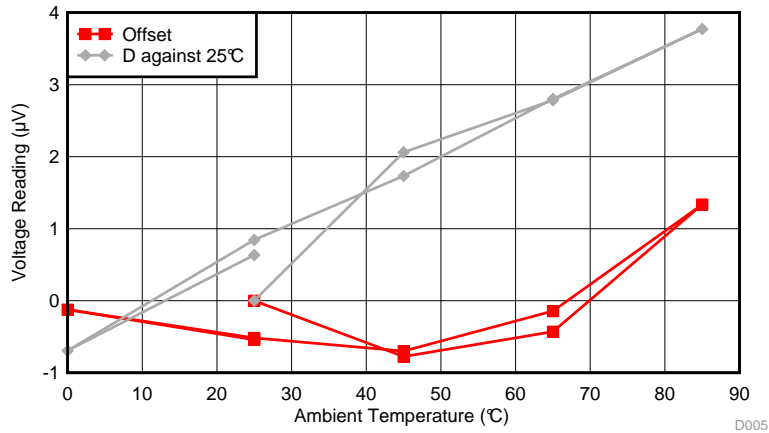
Figure 35. Error and Drift Over Temperature

8.2 Tests With Weight Scales on Food Processor

8.2.1 Resolution of Weight Measurement

To determine the TIDA-00765 board's performance towards a 1-g resolution, this test uses an off-the-shelf food processor with a 1-mV/V sensitivity of a single weight scale. There are three weight scales equipped to 3 feet of the food processor, which distribute the total weight by 1/3. The test is performed by placing a standard 1-g weight on top of the food processor and removing the standard weight repeatedly. Figure 36 shows the conversion results captured during the test.
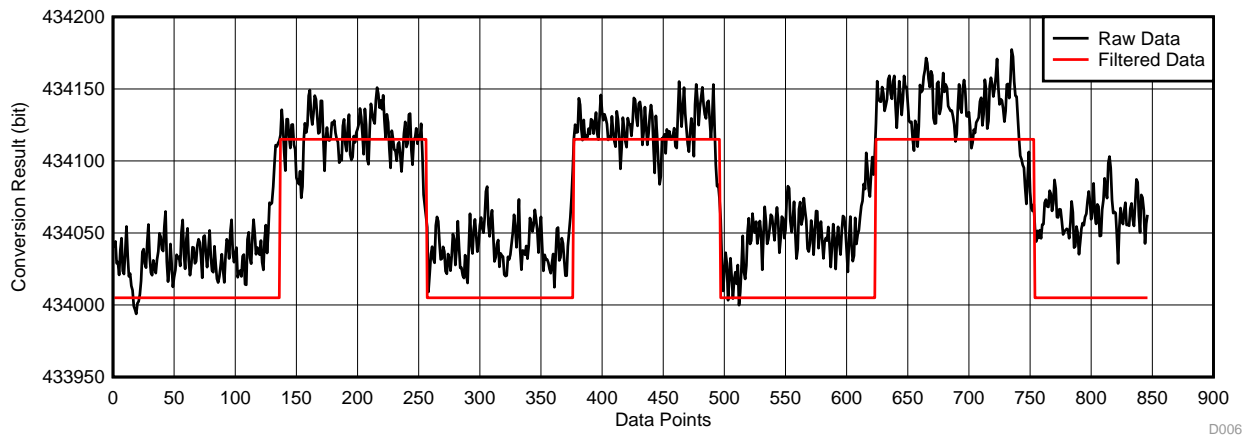
Figure 36. Conversion Results Raw and Filtered With 1-g Weight on Food Processor

In the test results shown in Figure 36, the peak-to-peak noise is much higher than using the test bridges on the TIDA-00765 board due to the mechanical vibration captured by the weight scale. However, with a sliding average of 16 sample points (8 with each polarity), a quantification with 55 (half the count is equivalent to 1 µV/g distributed to 3 feet), and a hysteresis of 55, the filtered data shown in Figure 36 illustrates that the resolution of the AFE of the TIDA-00765 can reach a 1-g stable reading with good repeatability.

The mechanical vibration from the food processor environment can introduce significant noise on the reading during weight measurement. Settings of the AFE for this test are:

- AC excitation with PGA gain of 128, normal operation mode with 20 SPS
- Three weight scales shorted together

8.2.2   Vibration Measurement With Food Processor

To capture the vibration status of the food processor during operation, 300-g apples cut into 1/8 pieces are used for the food processor to chop to generate vibration. Only one of the three weight scales is connected to the TIDA-00765 board through J3, and the ADS1220 is set to turbo mode with 2000 SPS and a PGA gain of 64. The motor of the food processor runs at a speed of 600 to 750 rpm. Figure 37 shows the conversion results in vibration measurement mode.
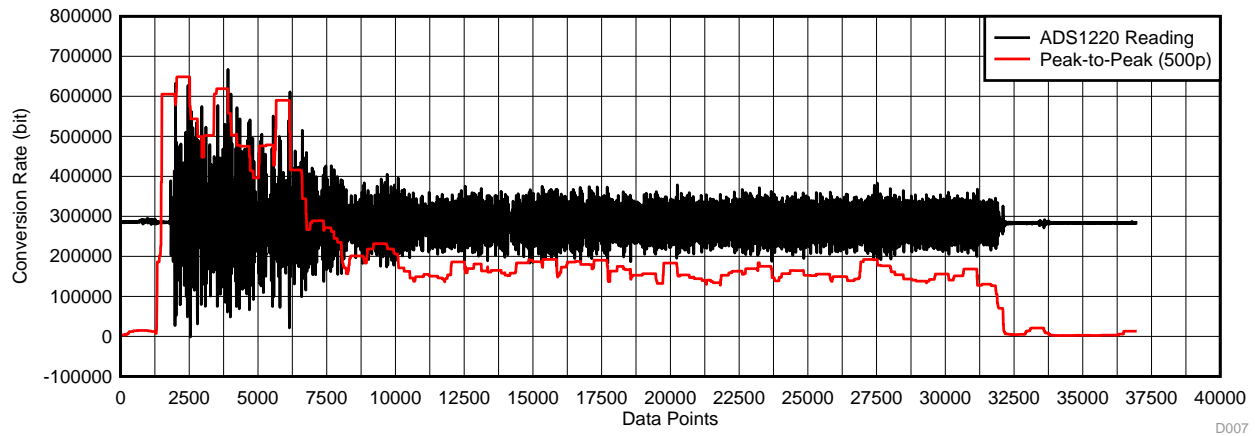
Figure 37. Conversion Results Raw and Peak-to-Peak of Vibration

From the test result, vibration status of the food processor during operation can be monitored over time by checking the peak-to-peak value of the conversion results. (In Figure 37, the peak-to-peak value is every 500 sample points).

By capturing the vibration status quickly, the application can keep vibrations within limit in case of unbalances to ensure safe yet effective operation, keep the level of audible noise reasonable, and detect and react to the progress of food processing.

Figure 38 and Figure 39 illustrate the relationship between the vibration level and the progress of food processing:
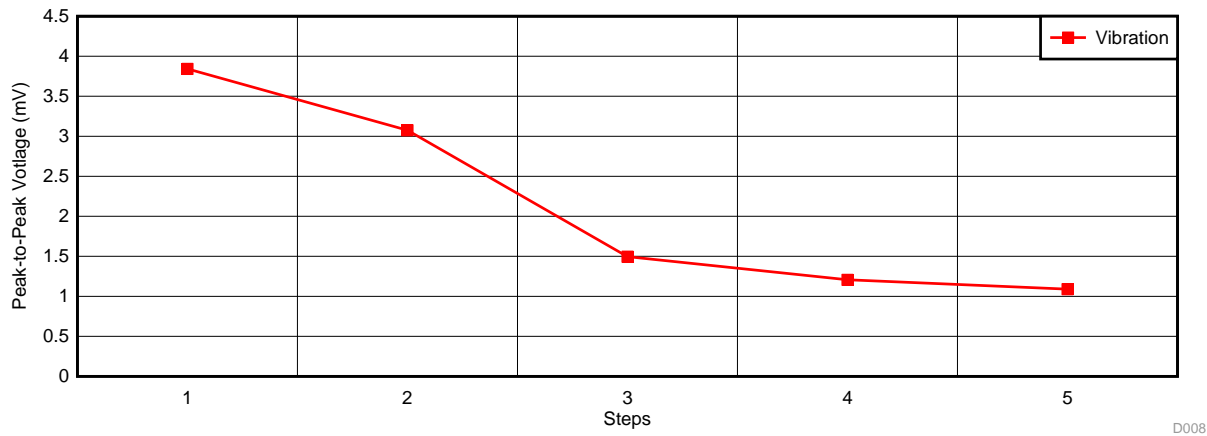
Figure 38. Vibration Level versus Progress of Food Processing

Step 0   Step 1   Step 2   Step 3   Step 4   Step 5

Figure 39. Visual Feedback of Vibration Level versus Progress of Food Processing

9   Design Files

9.1   Schematics

To download the schematics, see the design files at TIDA-00765.
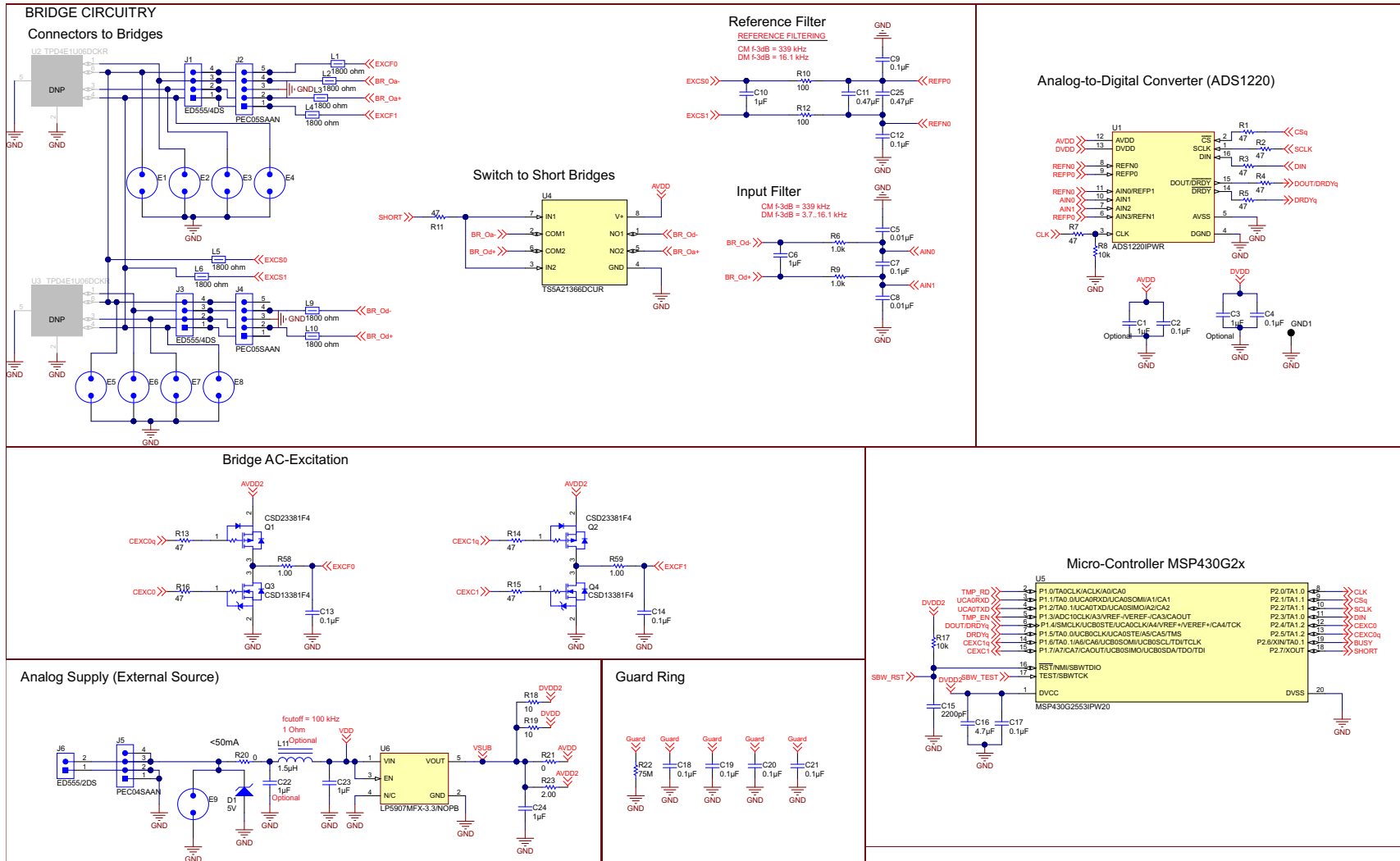
Figure 40. TIDA-00765 Main Board Schematic

TIDUBL0A–April 2016–Revised June 2016
Submit Documentation Feedback

1-g Resolution Over 15-kg Range Sub-100-nV$_{PP}$ Noise Front-End Reference   45
Design for Weight and Vibration Measurement

TEST AND DEBUG CIRCUITRY

Bridges Simulator
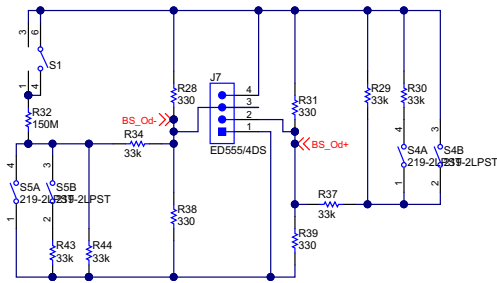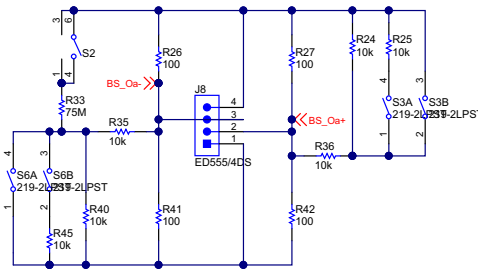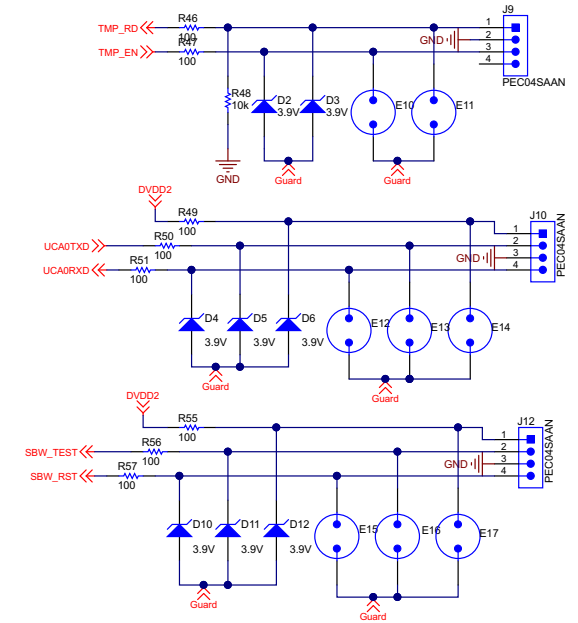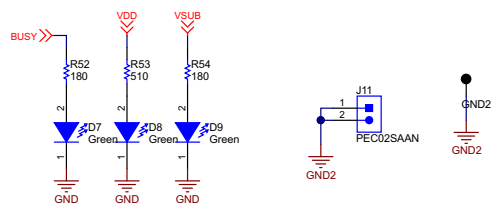
Figure 41. Test Board Schematic

46   *1-g Resolution Over 15-kg Range Sub-100-nV$_{PP}$ Noise Front-End Reference Design for Weight and Vibration Measurement*

TIDUBL0A−April 2016−Revised June 2016
Submit Documentation Feedback

9.2 Bill of Materials

To download the bill of materials (BOM), see the design files at TIDA-00765.

Table 9. BOM

ITEM	QTY	REFERENCE	VALUE	PART DESCRIPTION	MANUFACTURER	MANUFACTURER PARTNUMBER	PCB FOOTPRINT
1	1	!PCB1		Printed Circuit Board	Any	TIDA-00765	
2	7	C1, C3, C6, C10, C22, C23, C24	1uF	CAP, CERM, 1 µF, 25 V, +/- 10%, X7R, 0603	Kemet	C0603C105K3RACTU	0603
3	11	C2, C4, C7, C9, C12, C13, C14, C18, C19, C20, C21	0.1uF	CAP, CERM, 0.1 µF, 25 V, +/- 5%, X7R, 0603	Kemet	C0603C104J3RAC	0603
4	2	C5, C8	0.01uF	CAP, CERM, 0.01 µF, 50 V, +/- 5%, X7R, 0402	Kemet	C0402C103J5RACTU	0402
5	2	C11, C25	0.47uF	CAP, CERM, 0.47 µF, 16 V, +/- 10%, X7R, 0603	Kemet	C0603C474K4RACTU	0603
6	1	C15	2200pF	CAP, CERM, 2200 pF, 10 V, +/- 10%, X5R, 0402	MuRata	GRM155R61A222KA01D	0402
7	1	C16	4.7uF	CAP, CERM, 4.7 µF, 6.3 V, +/- 20%, X5R, 0402	MuRata	GRM155R60J475ME87D	0402
8	1	C17	0.1uF	CAP, CERM, 0.1 µF, 6.3 V, +/- 10%, X7R, 0402	MuRata	GRM155R70J104KA01D	0402
9	1	D1	5V	Diode, Zener, 20 V, 500 mW, SOD-123	Vishay-Semiconductor	MMSZ4707-V	SOD-123
10	8	D2, D3, D4, D5, D6, D10, D11, D12	3.9V	Diode, Zener, 3.9 V, 200 mW, SOD-323	Diodes Inc.	MMSZ5228BS-7-F	SOD-323
11	3	D7, D8, D9	Green	LED, Green, SMD	Wurth Elektronik	150060GS75000	LED_0603
12	0	FID1, FID2, FID3		Fiducial mark. There is nothing to buy or mount.	N/A	N/A	Fiducial
13	2	GND1, GND2	Black	Test Point, Miniature, Black, TH	Keystone	5001	Black Miniature Testpoint
14	4	H1, H2, H3, H4		Machine Screw, Round, #4-40 x 1/4, Nylon, Philips panhead	BandF Fastener Supply	NY PMS 440 0025 PH	Screw
15	4	H5, H6, H7, H8		Standoff, Hex, 0.5"L #4-40 Nylon	Keystone	1902C	Standoff
16	4	J1, J3, J7, J8		Terminal Block, 6A, 3.5mm Pitch, 4-Pos, TH	On-Shore Technology	ED555/4DS	14x8.2x6.5mm
17	2	J2, J4		Header, 2.54mm, 5x1, Tin, TH	Sullins Connector Solutions	PEC05SAAN	Header, 2.54mm, 5x1, TH
18	4	J5, J9, J10, J12		Header, 100mil, 4x1, Tin, TH	Sullins Connector Solutions	PEC04SAAN	Header, 4x1, 100mil, TH
19	1	J6		Terminal Block, 6A, 3.5mm Pitch, 2-Pos, TH	On-Shore Technology	ED555/2DS	7.0x8.2x6.5mm

TIDUBL0A–April 2016–Revised June 2016
Submit Documentation Feedback

1-g Resolution Over 15-kg Range Sub-100-nV$_{PP}$ Noise Front-End Reference 47
Design for Weight and Vibration Measurement

Table 9. BOM (continued)

ITEM	QTY	REFERENCE	VALUE	PART DESCRIPTION	MANUFACTURER	MANUFACTURER PARTNUMBER	PCB FOOTPRINT
20	1	J11		Header, 100mil, 2x1, Tin, TH	Sullins Connector Solutions	PEC02SAAN	Header, 2 PIN, 100mil, Tin
21	8	L1, L2, L3, L4, L5, L6, L9, L10	1800 ohm	Ferrite Bead, 1800 ohm @ 100 MHz, 0.1 A, 0402	MuRata	BLM15BD182SN1D	0402
22	1	L11	1.5uH	Inductor, Ferrite, 1.5 µH, 0.53 A, 0.22 ohm, SMD	MuRata	LQM18PN1R5MFH	0603
23	2	Q1, Q2	-12V	MOSFET, P-CH, -12 V, -2.3 A, YJC0003A	Texas Instruments	CSD23381F4	YJC0003A
24	2	Q3, Q4	12V	MOSFET, N-CH, 12 V, 2.1 A, YJC0003A	Texas Instruments	CSD13381F4	YJC0003A
25	11	R1, R2, R3, R4, R5, R7, R11, R13, R14, R15, R16	47	RES, 47, 5%, 0.063 W, 0402	Vishay-Dale	CRCW040247R0JNED	0402
26	2	R6, R9	1.0k	RES, 1.0 k, 5%, 0.063 W, 0402	Vishay-Dale	CRCW04021K00JNED	0402
27	3	R8, R17, R48	10k	RES, 10 k, 5%, 0.063 W, 0402	Vishay-Dale	CRCW040210K0JNED	0402
28	10	R10, R12, R46, R47, R49, R50, R51, R55, R56, R57	100	RES, 100, 5%, 0.063 W, 0402	Vishay-Dale	CRCW0402100RJNED	0402
29	2	R18, R19	10	RES, 10, 5%, 0.063 W, 0402	Vishay-Dale	CRCW040210R0JNED	0402
30	1	R20	0	RES, 0, 5%, 0.1 W, 0603	Vishay-Dale	CRCW06030000Z0EA	0603
31	1	R21	0	RES, 0, 5%, 0.063 W, 0402	Vishay-Dale	CRCW04020000Z0ED	0402
32	2	R22, R33	75Meg	RES, 75 M, 5%, 0.125 W, 0805	Stackpole Electronics Inc	HMC0805JT75M0	0805
33	1	R23	2.00	RES, 2.00, 1%, 0.063 W, 0402	Vishay-Dale	CRCW04022R00FKED	0402
34	6	R24, R25, R35, R36, R40, R45	10k	RES, 10 k, 0.01%, 0.125 W, 0805	Stackpole Electronics Inc	RNCF0805TKY10K0	0805
35	4	R26, R27, R41, R42	100	RES, 100, 0.02%, 0.1 W, 0805	Vishay Foil Resistors	Y1629100R000Q9R	0805
36	4	R28, R31, R38, R39	330	RES, 330, 0.01%, 0.1 W, 0805	Susumu Co Ltd	RG2012L-331-L-T05	0805
37	6	R29, R30, R34, R37, R43, R44	33k	RES, 33 k, 0.01%, 0.1 W, 0805	Susumu Co Ltd	URG2012L-333-L-T05	0805
38	1	R32	150Meg	RES, 150 M, 5%, 0.2 W, 0805	Stackpole Electronics Inc	HVCB0805JDD150M	0805
39	2	R52, R54	180	RES, 180, 5%, 0.063 W, 0402	Vishay-Dale	CRCW0402180RJNED	0402
40	1	R53	510	RES, 510, 5%, 0.063 W, 0402	Vishay-Dale	CRCW0402510RJNED	0402
41	2	R58, R59	1.00	RES, 1.00, 1%, 0.063 W, 0402	Vishay-Dale	CRCW04021R00FKED	0402
42	2	S1, S2		Switch, Toggle, SPST, 1Pos, TH	E-Switch	200USP9T1A1M2RE	Switch, 7.0x9.6x4.5mm
43	4	S3, S4, S5, S6		Switch, Slide, SPST 2 poles, SMT	CTS Electrocomponents	219-2LPST	2 poles SPST Switch
44	1	U1		Low-Power, Low-Noise, 24-Bit Analog-to-Digital Converter for Small Signal Sensors, PW0016A	Texas Instruments	ADS1220IPWR	PW0016A

48   *1-g Resolution Over 15-kg Range Sub-100-nV$_{PP}$ Noise Front-End Reference Design for Weight and Vibration Measurement*

TIDUBL0A–April 2016–Revised June 2016

Submit Documentation Feedback

Table 9. BOM (continued)

ITEM	QTY	REFERENCE	VALUE	PART DESCRIPTION	MANUFACTURER	MANUFACTURER PARTNUMBER	PCB FOOTPRINT
45	0	U2, U3		Quad Channel High Speed ESD Protection Device, DCK0006A	Texas Instruments	TPD4E1U06DCKR	DCK0006A
46	1	U4		0.75-Ohm DUAL SPST ANALOG SWITCH WITH 1.8-V COMPATIBLE INPUT LOGIC, DCU0008A	Texas Instruments	TS5A21366DCUR	DCU0008A
47	1	U5		16 MHz Mixed Signal Microcontroller with 16 KB Flash, 512 B SRAM and 24 GPIOs, -40 to 85 degC, 20-pin SOP (PW), Green (RoHS & no Sb/Br)	Texas Instruments	MSP430G2553IPW20	PW0020A
48	1	U6		ULTRA LOW-NOISE, 250-mA LINEAR REGULATOR FOR RF AND ANALOG CIRCUITS REQUIRES NO BYPASS CAPACITOR, DBV0005A	Texas Instruments	LP5907MFX-3.3/NOPB	DBV0005A

TIDUBL0A – April 2016 – Revised June 2016

1-g Resolution Over 15-kg Range Sub-100-nV$_{PP}$ Noise Front-End Reference Design for Weight and Vibration Measurement   49

Submit Documentation Feedback

9.3 *PCB Layout Recommendations*

The TIDA-00765 board consists of a two-layer layout with components on the top layer only. The two-layer design is one of the trade-offs of this design between the performance, size, and cost.

Pay attention to the following:

- High symmetry of the input and reference channels. This keeps noise pick-up symmetrical and ensures that the noise can be rejected by the good common rejection of the ADS1220.
- Separating aggressors such as frequent switching digital communication signals and sensitive analog input or reference signals during data captures. Spacing them apart from each other reduces both capacitive and other forms of coupling such as by reduced coupling capacitance.
- Filters were placed close to the analog inputs to minimize antennas and so noise coupling and sensitivity to interference pickup.
- At least one decoupling capacitor was placed in very close proximity of supply pins of devices to minimize the loop area, reduce the associated parasitic inductances, and maximize the efficiency of decoupling.
- An as solid as possible ground plane especially around the analog inputs, references, and below the ADS1220 to limit the loop area of return currents and noise pickup.
- If large cuts in the GND plane were unavoidable due to the two-layer board design, these cuts were bridge to reduce potential interferences. Especially return path areas for both digital and analog current loops need to be minimized.

Figure 42 shows the ground bridges added to gap the ground plane cutouts and consequently limit loop areas.
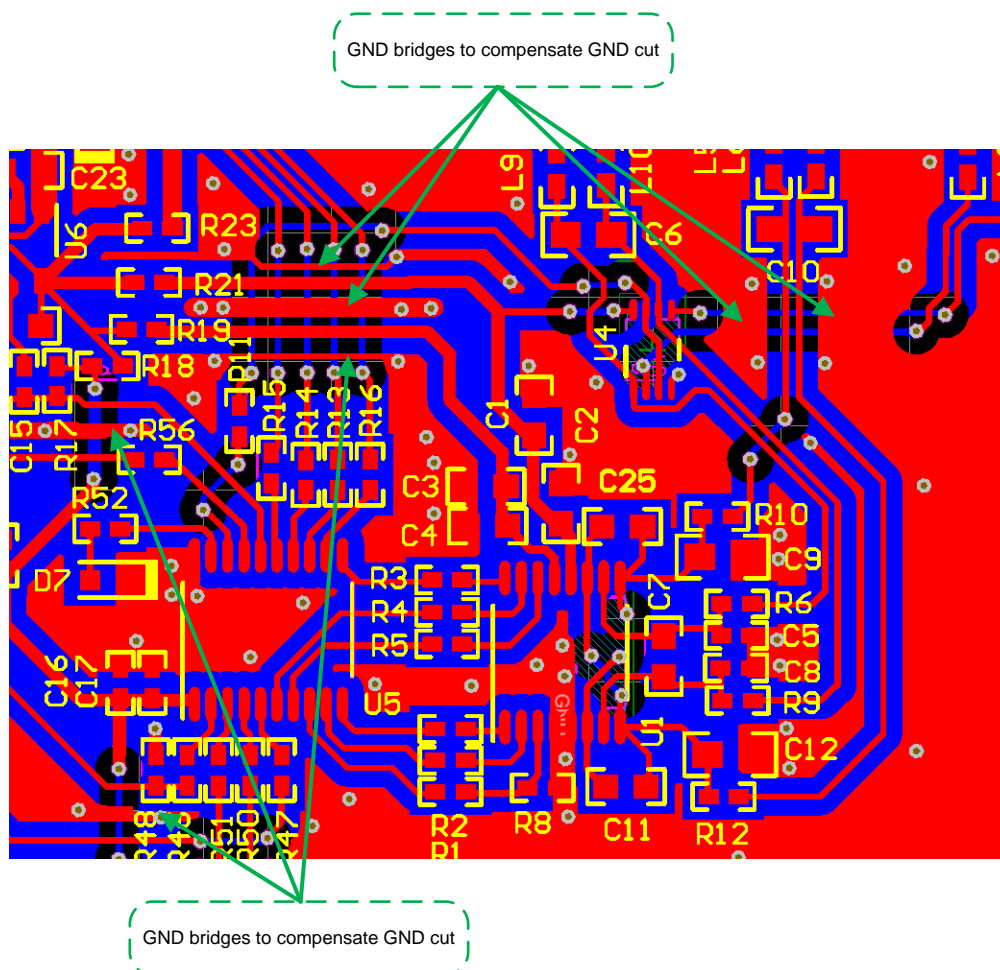
Figure 42. Layout Guidelines for GND Bridges

Copyright © 2016, Texas Instruments Incorporated
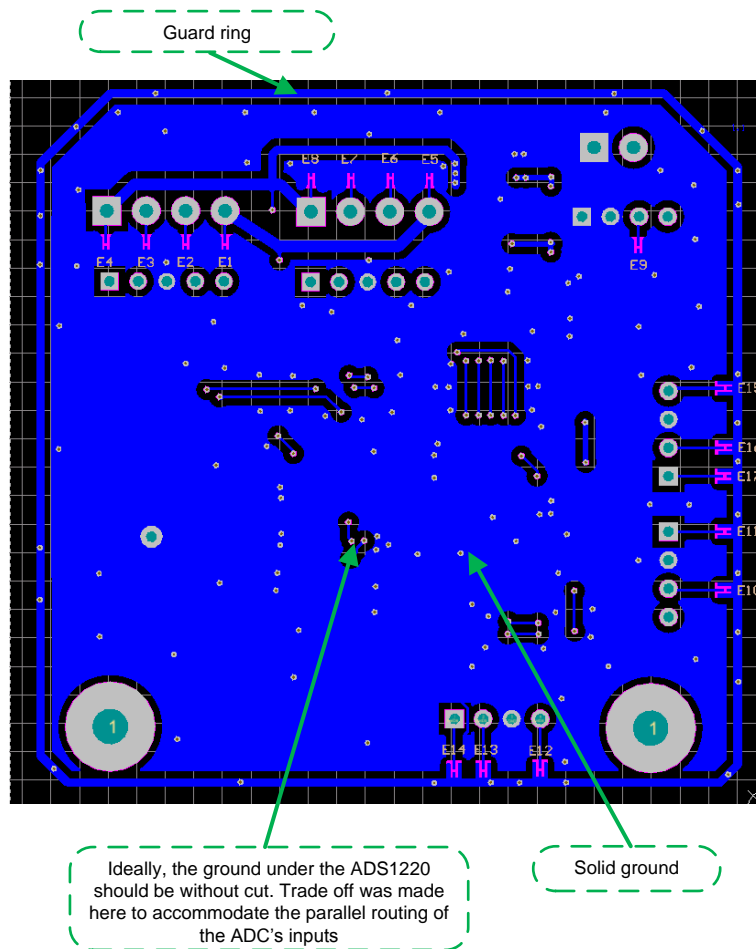
Figure 43. Layout Guidelines for Bottom Layer

Concerning the layout of the ADS1220, pay particular attention to the component placement and routing to minimize ground cuts. To use the internal MUX of the ADS1220 to reverse reference polarity, the reference signals need to cross each other; however, this requires cutting the ground plane below the ADS1220. This cut is undesirable, but it is the best compromise between board cost, return path minimization, and symmetry and close proximity of analog inputs and filters. This cut is highlighted on the bottom layer shown on Figure 43. If a four-layer board or external switches are used to reverse the polarity of the reference, this ground cut can be easily avoided.

As Figure 44 and Figure 45 show, place both the analog and digital the decoupling capacitors in very close proximity to the devices. This placement minimizes the supply current loop area for compensating currents, which then minimizes related parasitic inductances. Maximize the efficiency of decoupling minimizes the supply ringing and associated disturbances.
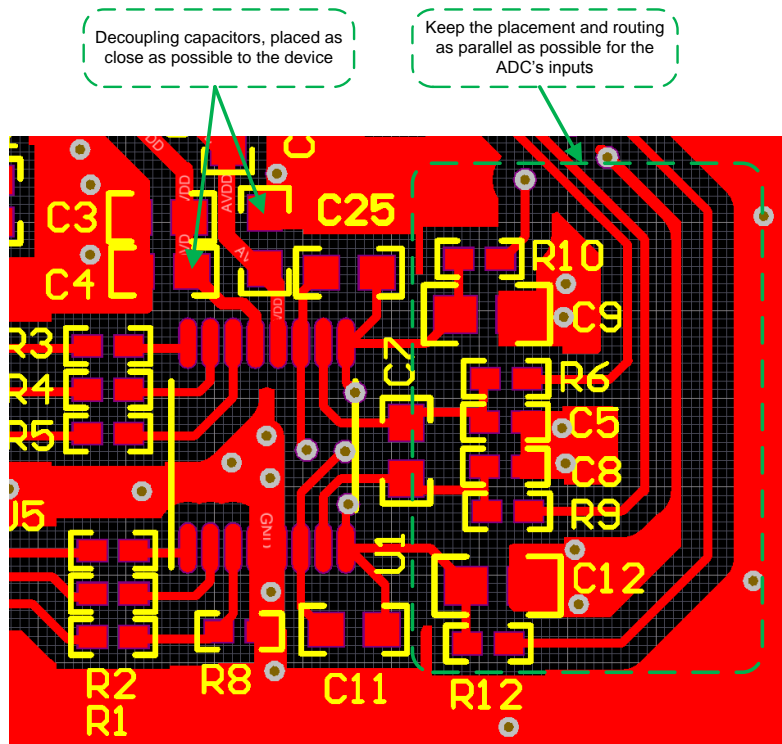
Figure 44. Layout Guidelines for ADS1220
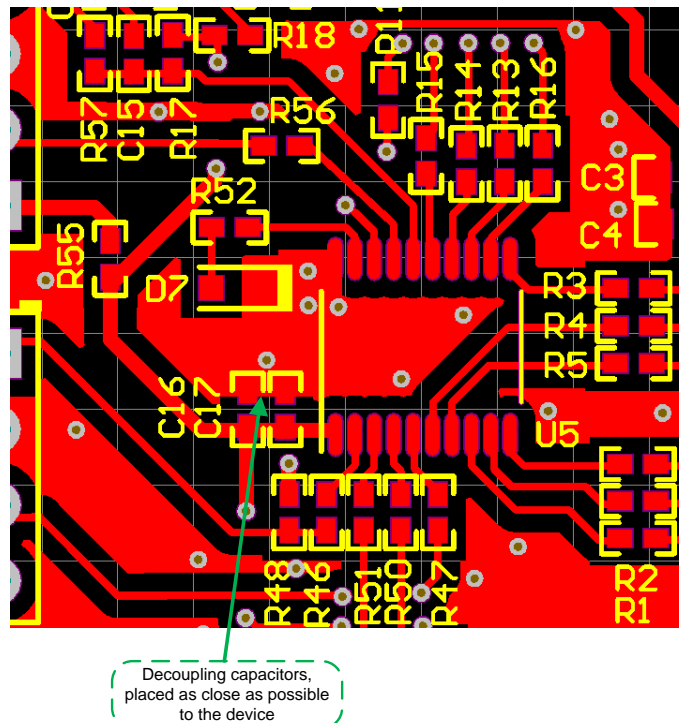
Figure 45. Layout Guidelines for MSP430G2553

The guard ring depicted in Figure 46 helps to separate grounds of protection devices connected to the digital interfaces and the ground of sensitive circuitry. It reduces noise and leakage pickup.
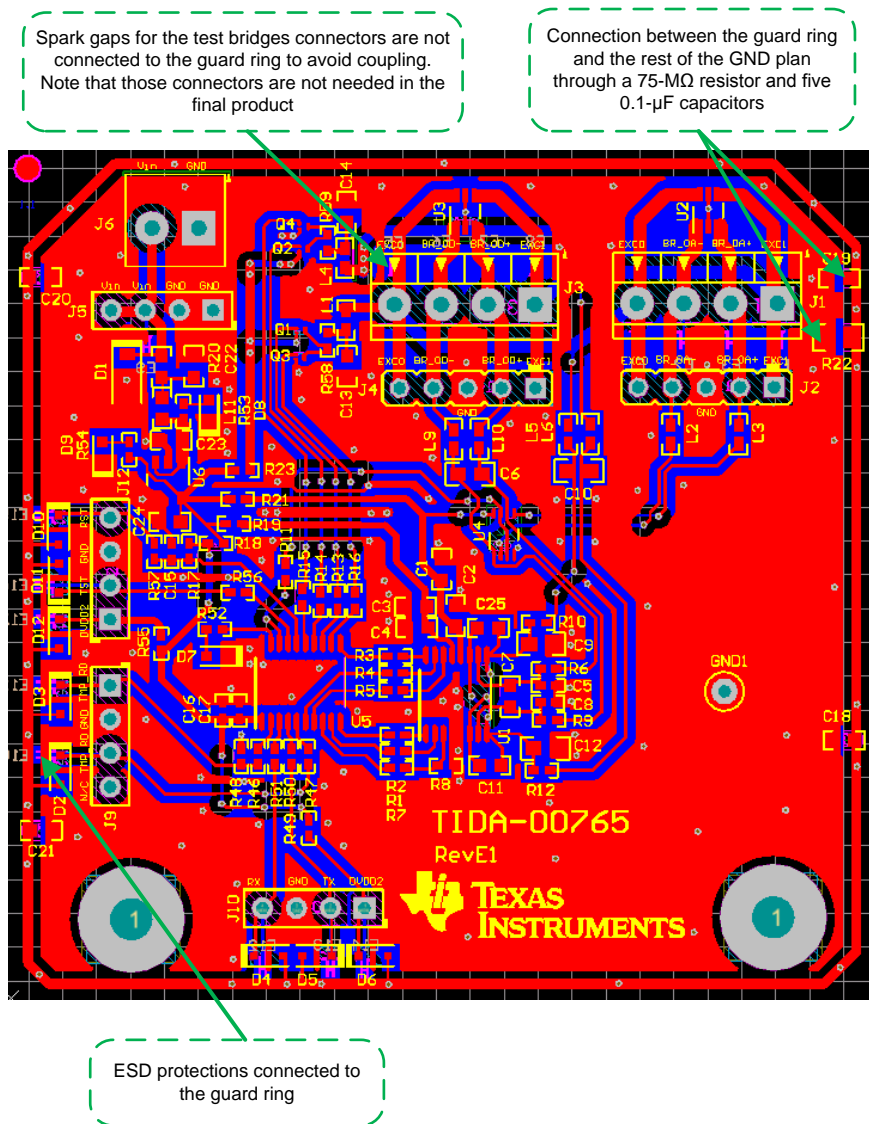
Figure 46. Layout Guidelines for ESD Protections

Copyright © 2016, Texas Instruments Incorporated

The layout of the test board contained in the TIDA-000765 is shown in Figure 47. It simulates a single resistive strain gage bridge and a parallel connection of multiple gages bridges. Add the board cutout to allow the two parts of the design to be separated, which is particular helpful to evaluate the temperature drift of the design.
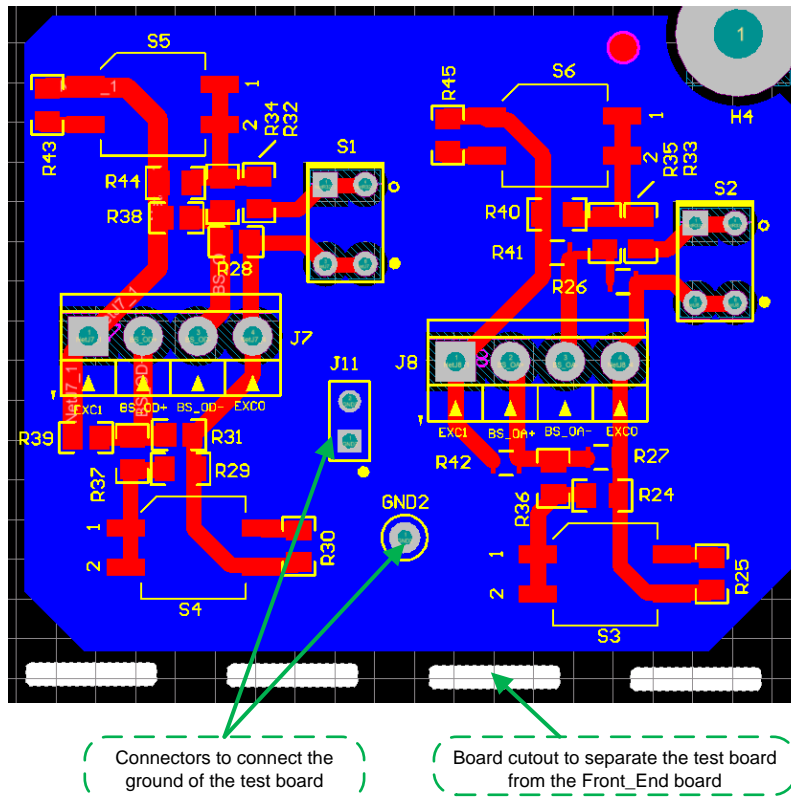
Figure 47. Layout Guidelines for Test Board

54   *1-g Resolution Over 15-kg Range Sub-100-nV$_{PP}$ Noise Front-End Reference Design for Weight and Vibration Measurement*

TIDUBL0A–April 2016–Revised June 2016
Submit Documentation Feedback

9.3.1 Layout Prints

To download the layer plots, see the design files at TIDA-00765.

href="Images/Layer_Top_Overlay_TIDUBL0.eps" scale="#IMPLIED"/
href="Images/Layer_Top_Solder_TIDUBL0.eps" scale="#IMPLIED"/
href="Images/Layer_Top_TIDUBL0.eps" scale="#IMPLIED"/ Figure 48. Top Overlay Figure 49. Top Solder
Mask Figure 50. Top Layer

href="Images/Layer_Bottom_TIDUBL0.eps" scale="#IMPLIED"/
href="Images/Layer_Bottom_Solder_TIDUBL0.eps" scale="#IMPLIED"/
href="Images/Layer_Bottom_Overlay_TIDUBL0.eps" scale="#IMPLIED"/ Figure 51. Bottom Layer
Figure 52. Bottom Solder Mask Figure 53. Bottom Overlay
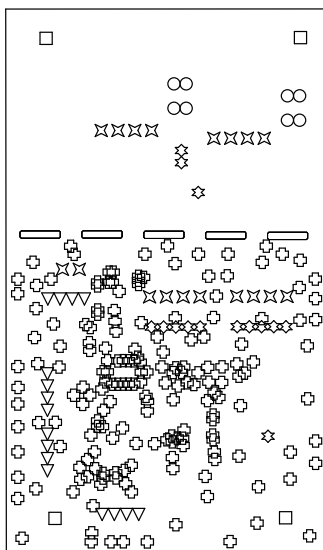
Symbol	Quantity	Finished Hole Size	Plated	Hole Type
✿	183	12.00mil (0.305mm)	PTH	Round
○	8	35.00mil (0.889mm)	PTH	Round
▽	16	39.37mil (1.000mm)	PTH	Round
✿	14	40.00mil (1.016mm)	PTH	Round
⋈	18	50.00mil (1.270mm)	PTH	Round
□	4	125.98mil (3.200mm)	PTH	Round
	243 Total			
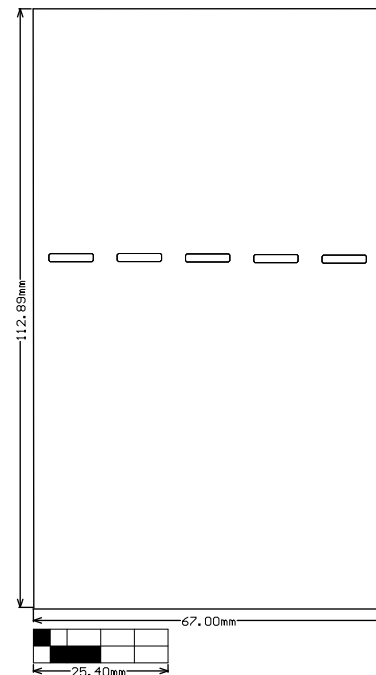
Figure 54. Drill Drawing

Figure 55. Board Dimensions

9.4 Altium Project

To download the Altium project files, see the design files at TIDA-00765.

9.5 Gerber Files

To download the Gerber files, see the design files at TIDA-00765.
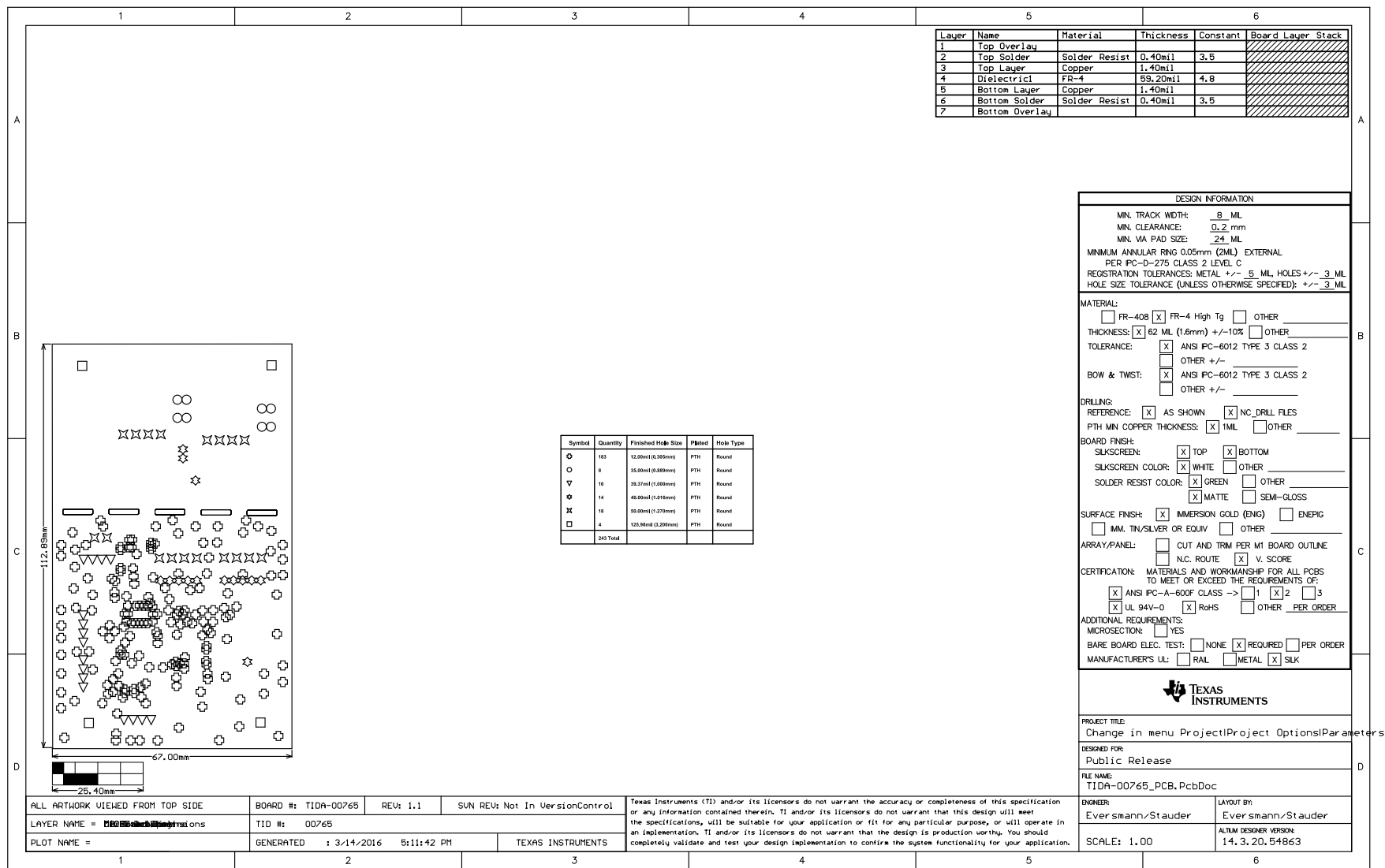
Figure 56. Fabrication Drawing

56   *1-g Resolution Over 15-kg Range Sub-100-nV$_{PP}$ Noise Front-End Reference
Design for Weight and Vibration Measurement*

TIDUBL0A–April 2016–Revised June 2016
Submit Documentation Feedback

9.6 Assembly Drawings

To download the assembly drawings, see the design files at TIDA-00765.
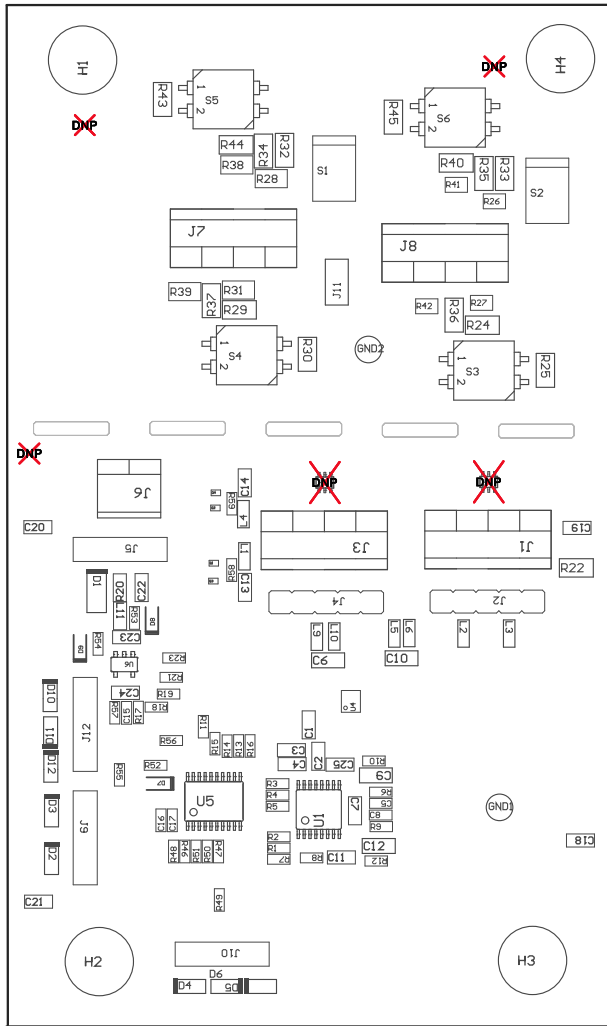
Figure 57. Top Assembly Drawing
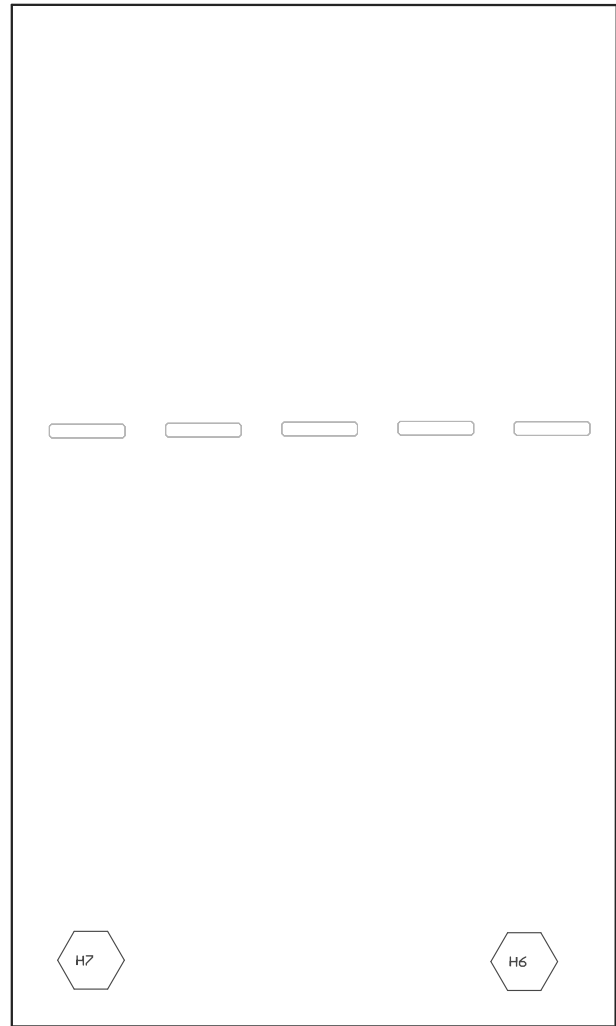
Figure 58. Bottom Assembly Drawing

TIDUBL0A–April 2016–Revised June 2016
Submit Documentation Feedback

1-g Resolution Over 15-kg Range Sub-100-nV$_{PP}$ Noise Front-End Reference Design for Weight and Vibration Measurement

57

10 Software Files

To download the software files, see the design files at TIDA-00765.

11 References

1. EDN Network, *Chopper op amps and noise*, May 03, 2013 (http://www.edn.com/electronics-blogs/the-signal/4413341/Chopper-op-amps-and-noise)
2. National Instruments, *Thermal EMF and Offset Voltage*, April 2010 (http://zone.ni.com/reference/en-XX/help/375472A-01/switch/thermal_voltages)
3. Texas Instruments, *Why should I give a flux?*, TI E2E Community (http://e2e.ti.com/blogs_/b/precisionhub/archive/2013/09/23/why-should-i-give-a-flux)
4. Texas Instruments, *ADS1220 Low-Power, Low-Noise, 24-Bit, ADC for Small-Signal Sensors*, ADS1220 Datasheet (SBAS501)
5. Texas Instruments, *High-Resolution, Low-Drift, Precision Weigh-Scale Reference Design with AC Bridge Excitation*, TIPD188 Design Guide (TIDUAC1)
6. Texas Instruments, *Precision Thermocouple Measurement with the ADS1118*, TIPD109 Design Guide (SLAU509)
7. Texas Instruments, *Thermocouple Analog Front End (AFE) Using RTD and Internal Temperature Sensor of ADS1220 for Cold Junction Compensation (CJC)*, TIDA-00168 Design Guide (TIDU574)
8. Texas Instruments, *RTD Ratiometric Measurements and Filtering Using the ADS1148 and ADS1248 Family of Devices*, ADS1220 Application Report (SBAA201)

12 About the Authors

Dr. BJOERN OLIVER EVERSMANN is a system architect in the Industrial Systems team at Texas Instruments, who is responsible for defining and implementing TI Designs for industrial applications.

RENTON MA is a system engineer in the Industrial Systems team at Texas Instruments, who is responsible for developing TI Designs for industrial applications.

KEVIN STAUDER is a system engineer in the Industrial Systems team at Texas Instruments, who is responsible for developing TI Designs for industrial applications.

The authors would like to give special recognition to the contributions from **JOACHIM WUERKER** and **BENJAMIN BOB** for their very helpful support.

58 *1-g Resolution Over 15-kg Range Sub-100-nV$_{PP}$ Noise Front-End Reference Design for Weight and Vibration Measurement*

TIDUBL0A−April 2016−Revised June 2016
Submit Documentation Feedback

Revision A History

NOTE: Page numbers for previous revisions may differ from page numbers in the current version.

Changes from Original (April 2016) to A Revision	**Page**
• Changed title	1
• Changed from preview page	1

IMPORTANT NOTICE FOR TI REFERENCE DESIGNS